Effectiveness of local unitary operations in n-local networks

Kaushiki Mukherjee *

Department of Mathematics, Government Girls' General Degree College, Ekbalpore, Kolkata 700023, India

(Received 19 September 2023; revised 19 December 2023; accepted 26 February 2024; published 19 March 2024)

Analyzing the nonclassicality of correlations generated in n-local quantum networks is an important branch of study in quantum information theory. Speaking of nonclassicality, violation of an n-local inequality ensures non n-locality of corresponding network correlations. Being correlation-based, violation of any such inequality is experimentally feasible. The present work explores whether applying suitable local unitary operations can aid violation of any n-local inequality. Observations have ensured the utility of local unitary operations in enhancing the detection efficiency of bilocal inequality and n-local inequality (for $n = 3, 4$) in the star configuration. In an n-local quantum network, such operations correspond to local basis change applied by at least one party over its joint state of qubits received from the sources. In an n-local network, with all the parties performing any possible local unitary operation, correlations not violating an n-local inequality (compatible with the network considered), are first characterized. Such characterization is then exploited to provide examples of local unitary operations aiding violation of existing n-local inequalities for $n = 2, 3$, and 4, specifically. Interestingly, there exist two qubit unitary operations, for which nontrilocal correlations can be simulated even when one of the sources distribute pure product state in star network. Quantum gates associated with the useful unitary operations are provided.

DOI: 10.1103/PhysRevA.109.032216

I. INTRODUCTION

The seminal work of Bell in 1964 [1] constitutes one of the most important ingredients in the development of quantum theory [1,2]. Violation of Bell's inequalities by any set of measurement correlations implies inexplicability of such set in terms of any physical model relying solely on local hidden variables. Such a type of correlation is commonly termed Bell nonlocal correlations and the corresponding experimental setup is usually known as a standard Bell experiment [3]. In such a scenario, a single source distributes particles between two or more distant parties

With increasing complexity in different correlations based practical tasks [4–7], it has become important to analyze quantum correlations arising in different network topologies. For past few years, study of nonlocality has thus undergone remarkable development beyond the purview of Bell scenario. In contrast with a standard Bell experimental setup, a network scenario involves multiple independent sources [8–10].

The assumption of source independence is significant in analyzing nonclassicality of network correlations. Such an assumption is often referred to as an n-local constraint [8,9] and an associated network is termed an n-local network (see Fig. 1). An n-local constraint helps in exploiting some novel features of multipartite nonlocality which cannot be witnessed in a standard Bell scenario. First, nonclassicality can be generated between parties who do not share any common past [9]. This phenomenon of generating nonclassicality among initially uncorrelated distant parties cannot be witnessed in any standard tripartite Bell scenario where nonlocality is obtained under the assumption that all the parties share a common past [3]. Second, non-n-locality can be observed when a subset or all the parties in the network performs fixed local measurement on their respective subsystems [9,11–14]. Such a measurement scenario is often referred to as a fixed input scenario [13] and the corresponding notion of nonclassicality as nonlocality without inputs [13]. This contributes to another interesting difference with multipartite Bell scenario where randomness in choice of local inputs by each party plays a crucial role in exploiting nonlocality [3].

Starting from the simplest network structure with two independent sources (bilocal network [8]), the study of the source-independence assumption has undergone multifaceted development, such as generalization of network structure in multiple aspects [11–13,15,16], framing closed forms of upper bound of violation of n-local inequalities [17,18], analysis of the concept of full network nonlocality [19], and many others [20–28]. In general, n-local networks are compatible with repeater networks [5–7] where entanglement distribution among initially uncorrelated nodes is based on entanglement swapping procedures. Hence, apart from theoretical significance, the study of non-n-locality is also important from experimental perspectives.

The nature of particles distributed by the sources along with local measurement contexts of the parties play a crucial role in exploiting non-n-locality in any network. Violation of an n-local inequality serves as a sufficient criterion to detect non-n-locality. In case all the sources distribute pure bipartite entangled states, under suitable local measurements, violation of n-local inequality is observed in both linear and nonlinear (star-shaped configuration) n-local networks [13,17]. However, if one of the sources sends two qubit product states, then no such violation is observed. If mixed entanglement

*kaushiki.wbes@gmail.com

distribution is considered, violation of n-local inequality is not always observed [17]. In this context, one may ask whether application of unitaries on the state of some of the particles distributed by the sources, aids for observing violation of an n-local inequality. The present discussion will provide an affirmative response to this query.

Over the past few years, the effect of unitary operations in exploiting Bell nonlocality has been studied [29–32]. Consider a bipartite state ρ_{AB} (say) shared between two parties Alice and Bob. Let ρ_{AB} not violate the Bell–Clauser-Horne-Shimony-Holt (Bell-CHSH) inequality [33] and therefore not be Bell-nonlocal in the two-input, two-output bipartite measurement scenario. Let Alice and Bob apply local unitary operations over their respective subsystems. The state ρ'_{AB} (say) obtained from ρ_{AB} under local basis change does not show any Bell-CHSH violation. However, if global unitary operation is applied over ρ_{AB}, the resulting state ρ''_{AB} (say) may show Bell-CHSH violation [30]. Application of suitable global unitary operations turn out to be useful in exploiting not only standard Bell nonlocality but also other forms of nonclassicality of bipartite states, such as entanglement [29], steering nonlocality, conditional negative entropy, and many others [31,32]. To this end, it may be noted that for applying global basis change on a bipartite state ρ_{AB}, both the particles forming the state and hence both Alice and Bob, sharing ρ_{AB}, must be at the same place. But under such circumstance, ρ_{AB} can be considered as a higher-dimensional single-particle state. Consequently, such a situation becomes incompatible for testing nonclassical features such as entanglement or any notion of nonlocality of a bipartite quantum state. In the current discussion, the effect of unitary operations in network scenario has been analyzed by avoiding such nonphysical situations.

Consider, for example, a bilocal network where each of two sources distribute a two-qubit state. Let each of the parties first apply local basis change on their respective subsystems and then perform local measurements (see Sec. III D). Corresponding tripartite correlations violate bilocal inequality [Eq. (8)]. It may be noted that violation of the same inequality is impossible if none of the parties apply a local basis change. Such an observation clearly points out the utility of applying suitable unitary operations locally by the parties. Specific instances are provided in support of this claim. Examples pointing out the effectiveness of local unitary operations are also obtained for the star network.

To explore the effect of unitary operations in exploiting non-n-local correlations, the notion of $\mathcal{I}_{\mathcal{T}}$-type absolute n-local correlations (see Sec. IV for details) has been introduced. The set of such correlations has been characterized. Given a specific network scenario with the independent sources generating a specific set of two qubit quantum states, the utility of unitary operations is implied by the simulation of correlations lying outside this set. Different examples pertaining to effectiveness of local unitary operations have been obtained in bilocal and star networks. Interestingly, on application of suitable local unitary operations, nontrilocal and also non 4-local correlations are generated in star network involving a two-qubit pure product state. The existing bilocal inequality [Eq. (8)] and trilocal inequality [Eq. (11)] become more resistant to noise when at least one of the parties in the network perform suitable local unitary operations. The effect of a local unitary operation can be realized by applying a reversible quantum gate [34]. Circuit implementation is provided for useful unitary operations.

The rest of the work is organized as follows: in Sec. II, the motivation of the present discussion is provided. In Sec. III, some prerequisites are given. Characterization of $\mathcal{I}_{\mathcal{T}}$-type absolute n-locality is provided in Sec. IV. The effect of unitary operations in aiding nonbilocality and nontrilocality detection is discussed in Sec. V. Resistance to noise is discussed in Sec. VI. Comparison between the present network scenario with that of the existing n-local networks is discussed in Sec. VII. Circuit implementation of the unitary operations used is provided in Sec. VIII. The discussion ends with some concluding remarks in Sec. IX.

II. MOTIVATION

Let ρ be a two-qubit entangled state shared between Alice and Bob in a standard bipartite Bell scenario [3]. Before performing measurements, Alice and Bob may apply local basis changes on their respective subsystems. Upon application of a suitable single-qubit unitary operation, the resulting measurement correlations may show Bell inequality violation [3]. Single-qubit unitary operations may thus help in exploiting Bell nonlocality in a standard Bell setup. Now, if ρ is Bell-CHSH local, then a violation of CHSH inequality is impossible irrespective of any single-qubit unitary operation applied by one or both of Alice and Bob on their respective share of ρ. However, from such a state, Bell nonlocality can still be exploited if ρ is subjected to a suitable two-qubit unitary operation [29]. Such a form of nonlocality is referred to as not absolute Bell-CHSH nonlocality and the two-qubit unitary as nonlocal unitary operation [29]. Application of two-qubits unitary operations may thus enhance violation of Bell inequality.

Now, for exploiting Bell nonlocality, the quantum state must be shared between physically distant parties. But, for applying a nonlocal unitary operation (global basis change), all parties must be in the same place, resulting in a nonphysical situation. This forms a major drawback in any study analyzing the effectiveness of two-qubit unitary operations in the standard Bell scenario. Such a compatibility issue can be avoided if one considers a quantum network structure. In a network, at least one of the parties, say $\mathcal{P}$, receives more than one qubit. $\mathcal{P}$ can now perform multiqubit unitary operations on the joint state of the subsystems received from multiple sources. Consequently, effectiveness of applying multiqubit unitary operations in exploiting nonclassicality can be tested in quantum networks. This motivates the entire discussion in the present work. To this end, it may be noted that the existing upper bounds of quantum violation of n-local inequalities in $\mathcal{N}_{\text{linear}}$ and $\mathcal{N}_{n\text{-star}}$ (see Sec. III for details) were derived under the assumption that the parties can perform single-qubit unitary operations prior to measurements. It thus becomes imperative to explore whether such bounds can be altered when any of the parties receiving more than one qubit performs multiqubit unitary operations. Although analysis of the n-local bounds in this context remains outside the scope of the

present discussion, the findings to be discussed in upcoming sections clearly ensure that such alternation is possible.

For analyzing the utility of applying multiqubit unitaries, the notion of $\mathcal{I}_{\mathcal{T}}$-type absolute n-locality will be introduced so as to categorize the entire set of network correlations from the perspective of n-local inequality $\mathcal{I}_{\mathcal{T}}$ violation (see Sec. IV). The utility of such a characterization is twofold: First, it helps to segregate quantum states which are useless in the sense that non-n-locality cannot be observed via violation of n-local inequality $\mathcal{I}_{\mathcal{T}}$ (compatible with $\mathcal{N}_{\mathcal{T}}$) even if all the parties perform all possible forms of local basis change (see Sec. IV A). Second, it points out the existence of two-qubit states which can show n-local inequality violation in the network only when the parties perform suitable unitary operations before measuring the states.

n-local networks form the basis of multiple practical tasks [4–7,35]. Due to the non-n-local feature of quantum correlations, quantum resources perform better than their classical counterparts in all such tasks [26]. With increasing development in technology, scalable quantum networks are now becoming practically implementable [5,7,36]. Now, violation of any n-local inequality detects non-n-local correlations. Being correlator-based, such a detection procedure is experimentally feasible. However, such detection criterion is only sufficient. Hence, non-n-local correlations may not always be detected. Consequently, quantum states used in the corresponding networks may seem useless. In this respect, it becomes important to search for any practically feasible procedure via which detection can be enhanced at least in some cases. Exploration for such procedures motivates the present discussion. It will be interesting to search for suitable multiqubit unitaries that will help in simulating more noise resistant quantum network correlations considering different types of noisy environments.

Before the onset of the main discussion, some basic ideas are discussed in the next section.

III. PRELIMINARIES

A. Density matrix representation of arbitrary two-qubit state

Let ϱ_{12} denote a two-qubit state. The density matrix of ϱ_{12} in terms of the Bloch sphere parameters is given by

$$\varrho_{12} = \frac{1}{4}\Bigg(\mathbb{I}_2 \times \mathbb{I}_2 + \vec{a}\cdot\vec{\sigma}\otimes\mathbb{I}_2 + \mathbb{I}_2\otimes\vec{b}\cdot\vec{\sigma} + \sum_{j_1,j_2=1}^{3} \mathfrak{w}_{j_1 j_2}\sigma_{j_1}\otimes\sigma_{j_2}\Bigg), \tag{1}$$

where $\vec{\sigma} = (\sigma_1, \sigma_2, \sigma_3)$, and σ_{j_k} labels Pauli operators along three mutually perpendicular directions ($j_k = 1, 2, 3$). $\vec{a} = (a_1, a_2, a_3)$ and $\vec{b} = (b_1, b_2, b_3)$ denote the local Bloch vectors ($\vec{a}, \vec{b} \in \mathbb{R}^3$) corresponding to party $\mathcal{A}$ and $\mathcal{B}$, respectively, with $|\vec{a}|, |\vec{b}| \leqslant 1$, and $(\mathfrak{w}_{i,j})_{3\times 3}$ denotes the correlation tensor $\mathcal{W}$(real). The matrix elements $\mathfrak{w}_{j_1 j_2}$ are given by $\mathfrak{w}_{j_1 j_2} = \mathrm{Tr}[\varrho_{12}\sigma_{j_1}\otimes\sigma_{j_2}]$.

On subjecting to suitable local unitary operations, $\mathcal{W}$ can be diagonalized [37,38]. The simplified expression is then given by [38]

$$\varrho'_{12} = \frac{1}{4}\Bigg(\mathbb{I}_2 \times \mathbb{I}_2 + \vec{\mathfrak{a}}\cdot\vec{\sigma}\otimes\mathbb{I}_2 + \mathbb{I}_2\otimes\vec{\mathfrak{b}}\cdot\vec{\sigma} + \sum_{j=1}^{3} \mathfrak{t}_{jj}\sigma_j\otimes\sigma_j\Bigg). \tag{2}$$

$T = \mathrm{diag}(\mathfrak{t}_{11}, \mathfrak{t}_{22}, \mathfrak{t}_{33})$ denotes the correlation matrix in Eq. (2) where $\mathfrak{t}_{11}, \mathfrak{t}_{22}, \mathfrak{t}_{33}$ are the eigenvalues of $(\mathcal{T}^T\mathcal{T})^{1/2}$, i.e., singular values of $\mathcal{T}$.

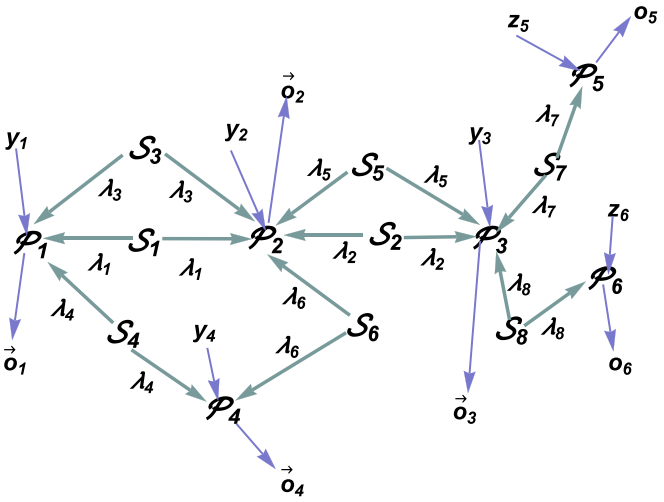

FIG. 1. Schematic diagram of a 5-local network. Each of $\mathcal{P}_1$, $\mathcal{P}_2$, $\mathcal{P}_3$, $\mathcal{P}_4$ is an intermediate party whereas $\mathcal{P}_5$ and $\mathcal{P}_6$ are both extreme parties. Inputs and outputs of these two types of parties are as detailed in Table I.

B. n-local networks

Consider a network involving n independent sources $\mathcal{S}_1, \mathcal{S}_2, \ldots, \mathcal{S}_n$ and $n+1$ parties $\mathcal{P}_1, \mathcal{P}_2, \ldots, \mathcal{P}_{n+1}$ (for example, see Fig. 1). For all j, let $\mathcal{S}_j$ distribute physical systems to two parties $\mathcal{P}_j$ and $\mathcal{P}_{j'}$ ($j, j' \in \{1, 2, \ldots, n+1\}$). The network is referred to as an $n-$*local network* [26]. Such a network (for example, see Fig. 1) can be of any configuration. Let $\mathcal{N}_{\mathcal{T}}$ denote an n-local network having configuration $\mathcal{T}$ (say). Depending on the number of particles received from

TABLE I. For any party $\mathcal{P}_j$ ($j \in \{1, 2, \ldots, n+1\}$) in $\mathcal{N}_{\mathcal{T}}$, details of the input and outputs are enlisted here.

Type	No. of particles received	Inputs and Outputs
Extreme	Single	Chooses an input from two dichotomous inputs $z_j \in \{0, 1\}$. outputs are binary valued denoted as $o_j \in \{\pm 1\}$.
Intermediate	m (say) $2 \leqslant m \leqslant n$	Single input y_j having m binary valued outputs labeled as a string: $\vec{\mathbf{o}}_j = (o_j^{(1)}, o_j^{(2)}, ..., o_j^{(m)})$ with $o_j^{(k)} \in \{\pm 1\}$.

the sources, the parties are of two types: intermediate and extreme. Details of these two types of parties are provided in Table I.

The source-independence criterion is given by the n-local constraint [9]:

$$\chi(\lambda_1, \lambda_2, \ldots, \lambda_n) = \Pi_{j=1}^{n} \chi_j(\lambda_j), \tag{3}$$

where, for all j, λ_j denotes the hidden variable characterizing the physical system generated from $\mathcal{S}_j$ and χ_j denotes the normalized distribution of λ_j.

$(n+1)$-partite measurement correlations are local if

$$P\left(o_{i_1}, o_{i_2}, \ldots, o_{i_r}, \bar{\mathbf{o}}_{j_1}, \bar{\mathbf{o}}_{j_2}, \ldots, \bar{\mathbf{o}}_{j_{r'}} | z_{i_1}, z_{i_2}, \ldots, z_{i_r}, y_{j_1}, y_{j_2}, \ldots, y_{j_{r'}}\right) = \int_{\Lambda_1}\int_{\Lambda_2}\ldots\int_{\Lambda_n} d\lambda_1 d\lambda_2 \ldots d\lambda_n \chi(\lambda_1, \lambda_2, \ldots \lambda_n)\mathbf{P}, \tag{4}$$

with $\mathbf{P} = \Pi_{s=1}^{r} P(o_{i_s}|z_{i_s}, \lambda_{i_s})\Pi_{t=1}^{r'} P(\bar{\mathbf{o}}_{j_t}|y_{j_t}, \bar{\mathbf{L}}_{\mathbf{t}})$, where $1 \leqslant r, r' \leqslant n+1$ such that $r + r' = n+1$ for all s and t, indices $i_s, j_t \in \{1, 2, \ldots, n+1\}$, and

$$\bar{\mathbf{L}}_{\mathbf{t}} = \left(\lambda_{p_1}, \lambda_{p_2}, \ldots, \lambda_{p_m}\right) \subset \{\lambda_1, \ldots, \lambda_n\}, \tag{5}$$

such that each of $\mathcal{S}_{p_1}, \mathcal{S}_{p_2}, \ldots, \mathcal{S}_{p_m}$ sends particles to $\mathcal{P}_{j_t}$. $(n+1)$-partite correlations that satisfy both Eqs. (3) and (4) are termed n-local correlations. So, any set of correlations that do not satisfy Eqs. (3) and (4) simultaneously are termed non-n-local [9].

Let P_{n+1} denote the set of measurement correlation terms generated in $\mathcal{N}_{\mathcal{T}}$. Consider the inequality

$$f(P_{n+1}) \leqslant 1, \tag{6}$$

where $f(.)$ denotes any function of the correlation terms in $\mathcal{N}_{\mathcal{T}}$. If any set of n-local correlations in $\mathcal{N}_{\mathcal{T}}$ satisfy Eq. (6), then this inequality is referred to as an n-local inequality. Violation of Eq. (6) thus acts as a sufficient criterion to detect the non-n-local nature of corresponding correlations (P_{n+1}) in $\mathcal{N}_{\mathcal{T}}$.

C. Quantum n-local networks [26]

For all $i = 1, 2, \ldots, n$, let $\mathcal{S}_i$ distribute a two-qubit state $\varrho_{i,i+1}$. Let ρ_{in} denote the overall state in the network:

$$\rho_{\text{in}} = \otimes_{j=1}^{n} \rho_{j,j+1}. \tag{7}$$

As discussed in Table I, for any $j \in \{1, 2, \ldots, n+1\}$, $\mathcal{P}_j$ receives m qubits where $m = 1$ $(2 \leqslant m \leqslant n)$ if $\mathcal{P}_j$ is an extreme (intermediate) party in $\mathcal{N}_{\mathcal{T}}$. Let an extreme party perform projective measurement in any one of two arbitrary directions whereas an intermediate party performs single projective measurements in a basis $\mathfrak{B}$ (say) of m qubits [26]. Let $\mathcal{M}_j$ denote the local measurement of $\mathcal{P}_j$ $\forall$ $j = 1, 2, \ldots, n+1$.

Two specific n-local networks of different configurations are discussed next.

D. Linear n-local network [11]

n independent sources and $n+1$ parties are arranged in a linear pattern (see Fig. 2). Let the network be denoted by $\mathcal{N}_{\text{linear}}$. Here $\mathcal{P}_2, \mathcal{P}_3, \ldots, \mathcal{P}_{n-1}$ are the intermediate parties and $\mathcal{P}_1, \mathcal{P}_{n+1}$ are the extreme parties. $(n+1)$-partite correlations are n-local if those satisfy both Eqs. (3) and (4). So, any set of $(n+1)$-partite correlations not satisfying both restrictions (3) and (4) are termed non-n-local. The existing n-local inequality is given by [11]

$$\begin{aligned}
&\sqrt{|I_n|} + \sqrt{|J_n|} \leqslant 1, \text{ where} \\
&I_n = \frac{1}{4}\sum_{y_1, y_{n+1}} \left\langle O_{1,y_1} O_2^0 O_3^0 \ldots O_{n-1}^0 O_{n+1,y_{n+1}} \right\rangle, \\
&J_n = \frac{1}{4}\sum_{y_1, y_{n+1}} (-1)^{y_1+y_{n+1}} \left\langle O_{1,y_1} O_2^1 O_3^1 \ldots O_{n-1}^1 O_{n+1,y_{n+1}} \right\rangle, \text{ with} \\
&\left\langle O_{1,y_1} O_2^i O_3^i \ldots O_{n-1}^i O_{n+1,y_{n+1}} \right\rangle = \sum_{\mathcal{D}_1} (-1)^{\mathbf{o}_1 + \mathbf{o}_{n+1} + \sum_{j=2}^{n-1} \mathbf{o}_{jk}} N_1, \\
&\text{where } N_1 = p(\mathbf{o}_1, \bar{\mathbf{o}}_2, \ldots, \bar{\mathbf{o}}_{n-1}\mathbf{o}_{n+1} | y_1, y_{n+1}, z_2, \ldots, z_n), \\
&i = 0, 1, \\
&k = i+1 \text{ and } \mathcal{D}_1 = \{\mathbf{o}_1, \mathbf{o}_{21}, \mathbf{o}_{22}, \ldots, \mathbf{o}_{(n-1)1}, \mathbf{o}_{(n-1)2}\mathbf{o}_{n+1}\}.
\end{aligned} \tag{8}$$

Violation of Eq. (8) guarantees that the corresponding correlations are non-n-local. Equation (8) being a sufficient criterion, no definite conclusion can be given if this inequality is satisfied.

Now, for all i, let $\mathcal{S}_i$ distribute an arbitrary two-qubit state $\rho_{i,i+1}$ [Eq. (2)]. Let each of $n-1$ intermediate parties perform Bell basis measurements [9]. As discussed in Sec. III C, each of the two extreme parties performs projective measurements. To be precise, $\mathcal{P}_1$ performs any one of $\vec{m}_0 \cdot \vec{\sigma}$, $\vec{m}_1 \cdot \vec{\sigma}$ and similarly $\mathcal{P}_{n+1}$ performs any one of $\vec{n}_0 \cdot \vec{\sigma}$, $\vec{n}_1 \cdot \vec{\sigma}$ In such measurement context, the upper bound of Eq. (8) is given by [17] $(\Pi_{j=1}^{n} t_{j11} + \Pi_{j=1}^{n} t_{j22})^{1/2}$, where t_{j11}, t_{j22} are the largest two singular values of correlation tensor (T_j, say) of $\rho_{j,j+1}$ $(j = 1, \ldots, n)$. The n-local inequality (8) is thus violated if

$$\sqrt{\Pi_{j=1}^{n} t_{j11} + \Pi_{j=1}^{n} t_{j22}} > 1. \tag{9}$$

So, if Eq. (9) is not satisfied, then corresponding tripartite correlations turn out to be n-local as per the n-local inequality [Eq. (8)]. For the present purpose, the above inequality for

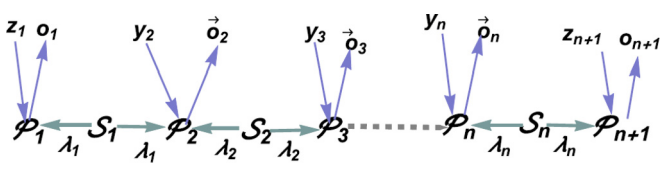

FIG. 2. Schematic diagram of an n-local linear network ($\mathcal{N}_{\text{linear}}$).

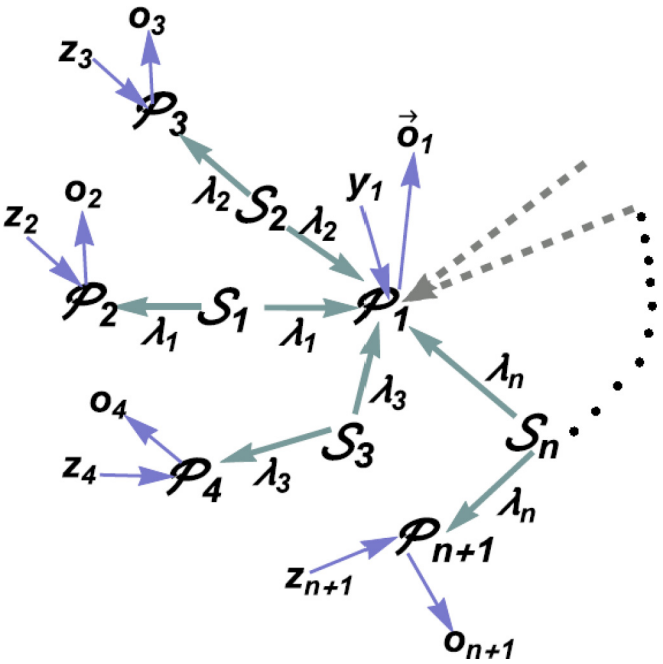

FIG. 3. Schematic diagram of an n-local nonlinear network in the star configuration ($\mathcal{N}_{n\text{-star}}$).

$n = 2$ will be used:

$$\sqrt{\Pi_{j=1}^{2} t_{j11} + \Pi_{j=1}^{2} t_{j22}} > 1. \tag{10}$$

E. Star network [12]

The star network is a nonlinear n-local network consisting of a single intermediate party (often referred to as the central party) $\mathcal{P}_1$ and n extreme parties $\mathcal{P}_2, \ldots, \mathcal{P}_{n+1}$ (see Fig. 3). Let the network be denoted by $\mathcal{N}_{n\text{-star}}$. $(n+1)$-partite correlations are said to be n-local if those satisfy both Eqs. (3) and (4). So, any set of $(n+1)$-partite correlations not satisfying both of these restrictions [Eqs. (3) and (4)], are termed non-n-local. The existing n-local inequality for $\mathcal{N}_{n\text{-star}}$ is given by [17]

$$\sum_{i=1}^{2^{n-1}} |J_i|^{\frac{1}{n}} \leqslant 2^{n-2}, \text{ where} \tag{11}$$

$$J_i = \frac{1}{2^n} \sum_{y_2,\ldots,y_{n+1}} (-1)^{h_i(y_2,\ldots,y_{n+1})} \left\langle A_{(1)}^{(i)} A_{y_2}^{(2)} \ldots A_{y_{n+1}}^{(n+1)} \right\rangle,$$

$$\left\langle A_{(1)}^{(i)} A_{y_2}^{(2)} \ldots A_{y_{n+1}}^{(n+1)} \right\rangle = \sum_{\mathcal{D}_2} (-1)^{\tilde{\mathfrak{o}}_1^{(i)} + \mathbf{o}_2 + \ldots + \mathbf{o}_{n+1}} N_2, \tag{12}$$

where $N_2 = p(\overline{\mathbf{o}}_1, \mathbf{o}_2, \ldots, \mathbf{o}_{n+1} | z_1, y_2, \ldots, y_{n+1})$, $j = 1, \ldots, n$, and $\mathcal{D}_2 = \{\mathbf{o}_{11}, \ldots, \mathbf{o}_{1n}\mathbf{o}_2, \ldots, \mathbf{o}_{n+1}\}$.

In Eq. (11), for all $i = 1, 2, \ldots, 2^{n-1}$, $\tilde{\mathfrak{o}}_1^{(i)}$ represents an output bit generated by classical postprocessing of the raw output string $\overline{\mathbf{o}_1} = (\mathbf{o}_{11}, \ldots, \mathbf{o}_{1n})$ of $\mathcal{P}_1$. In Eq. (11), for all i, h_i are functions of the input variables $y_2, \ldots, y_{n+1}$ of the extreme parties [12]. Each h_i contains an even number of $y_2, \ldots, y_{n+1}$. For $n = 3, 4$, classical postprocessed bits $\tilde{\mathfrak{o}}_1^{(i)}$ from the output string $\overline{\mathbf{o}_1}$ and corresponding functions $h_i(y_2, y_3, \ldots, y_{n+1})$ are specified in Table II.

TABLE II. Details of the classically postprocessed bits $\tilde{\mathfrak{o}}_1^{(i)}$ and the functions $h_i(y_2, y_3, \ldots, y_{n+1})$ for $n = 3, 4$ in Eq. (11).

n	$\tilde{\mathfrak{o}}_1^{(i)}$	$h_i(y_2, y_3, ..., y_{n+1})$
3	$\tilde{\mathfrak{o}}_1^{(1)} = \mathbf{o}_{11}$, $\tilde{\mathfrak{o}}_1^{(2)} = \mathbf{o}_{11} \oplus \mathbf{o}_{12} \oplus 1$	$h_1 = 0, h_2 = y_2 + y_3$
	$\tilde{\mathfrak{o}}_1^{(3)} = \mathbf{o}_{11} \oplus \mathbf{o}_{13} \oplus 1$	$h_3 = y_2 + y_4$
	$\tilde{\mathfrak{o}}_1^{(4)} = \mathbf{o}_{11} \oplus \mathbf{o}_{12} \oplus \mathbf{o}_{13} \oplus 1$	$h_4 = y_3 + y_4$
4	$\tilde{\mathfrak{o}}_1^{(1)} = \mathbf{o}_{11}$, $\tilde{\mathfrak{o}}_1^{(2)} = \mathbf{o}_{11} \oplus \mathbf{o}_{12} \oplus 1$	$h_1 = 0, h_2 = y_2 + y_3$
	$\tilde{\mathfrak{o}}_1^{(3)} = \mathbf{o}_{11} \oplus \mathbf{o}_{13} \oplus 1$	$h_3 = y_2 + y_4$
	$\tilde{\mathfrak{o}}_1^{(4)} = \mathbf{o}_{11} \oplus \mathbf{o}_{14} \oplus 1$	$h_4 = y_2 + y_5$
	$\tilde{\mathfrak{o}}_1^{(5)} = \mathbf{o}_{11} \oplus \mathbf{o}_{12} \oplus \mathbf{o}_{13} \oplus 1$	$h_5 = y_3 + y_4$
	$\tilde{\mathfrak{o}}_1^{(6)} = \mathbf{o}_{11} \oplus \mathbf{o}_{12} \oplus \mathbf{o}_{14} \oplus 1$	$h_6 = y_3 + y_5$
	$\tilde{\mathfrak{o}}_1^{(7)} = \mathbf{o}_{11} \oplus \mathbf{o}_{14} \oplus \mathbf{o}_{13} \oplus 1$	$h_7 = y_4 + y_5$
	$\tilde{\mathfrak{o}}_1^{(8)} = \mathbf{o}_{11} \oplus \mathbf{o}_{12} \oplus \mathbf{o}_{13} \oplus \mathbf{o}_{14}$	$h_8 = y_2 + y_3 + y_4 + y_5$

Let each of the n independent sources distribute an arbitrary two-qubit state [Eq. (2)]. Let $\mathcal{P}_1$ perform Greenberger-Horne-Zeilinger (GHZ) basis measurements [12]. Each of the extreme parties performs projective measurements. In such a measurement context, the upper bound of Eq. (11) is given by [18] $[(\Pi_{j=1}^{n} t_{j11})^{\frac{2}{n}} + (\Pi_{j=1}^{n} t_{j22})^{\frac{2}{n}}]^{1/2}$. The n-local inequality [Eq. (11)] is thus violated if

$$2^{n-2} \sqrt{\left(\Pi_{j=1}^{n} t_{j11}\right)^{\frac{2}{n}} + \left(\Pi_{j=1}^{n} t_{j22}\right)^{\frac{2}{n}}} > 2^{n-2}. \tag{13}$$

So, if Eq. (13) is not satisfied, then the corresponding $(n+1)$-partite correlations turn out to be n-local, as per the n-local inequality [Eq. (11)]. For present discussion, mainly the upper bound of Eq. (11) in $\mathcal{N}_{3\text{-star}}$ and $\mathcal{N}_{4\text{-star}}$ will be used:

$$2\sqrt{\left(\Pi_{j=1}^{3} t_{j11}\right)^{\frac{2}{3}} + \left(\Pi_{j=1}^{3} t_{j22}\right)^{\frac{2}{3}}} > 2, \tag{14}$$

$$4\sqrt{\left(\Pi_{j=1}^{4} t_{j11}\right)^{\frac{1}{2}} + \left(\Pi_{j=1}^{4} t_{j22}\right)^{\frac{1}{2}}} > 4. \tag{15}$$

F. Application of unitary operations

Let $\varrho_{1,2}$ denote a two-qubit state. In general, the application of a qubit unitary operation on $\varrho_{1,2}$ consists in applying single-qubit unitary operations separately on each of the two qubits and a two-qubit unitary operation on the joint state of both qubits [38]. A single unitary operation, say $L(\theta, \vec{\eta}\,)$ or simply L corresponds to rotation of a qubit through an angle θ about any axis $\vec{\eta} = (\eta_1, \eta_2, \eta_3)$. The general form of such a unitary operation is given by [38]

$$L = \cos\left(\frac{\theta}{2}\right)\sigma_0 - i \sin\left(\frac{\theta}{2}\right) \sum_{i=1}^{3} \eta_i \sigma_i, \quad \eta_i \in \Re. \tag{16}$$

Let $U(\phi_1, \phi_2, \phi_3)$ denote a 4×4 unitary matrix. Such a matrix corresponds to a two-qubit unitary operation. Three specific forms of two-qubit unitary operations will be used in the present discussion. These are listed below:

$$U(\phi_1, \phi_2, \phi_3) = \Pi_{i=1}^{3} (\cos\phi_i \sigma_0 \otimes \sigma_0 - i \sin\phi_i \sigma_i \otimes \sigma_i),$$
$$\phi_i \in \Re, \tag{17}$$

$$U(\beta_1,\beta_2,\beta_3) = (\cos\beta_1\sigma_0\otimes\sigma_0 - i\sin\beta_1\sigma_1\otimes\sigma_2),$$
$$(\cos\beta_2\sigma_0\otimes\sigma_0 - i\sin\beta_2\sigma_2\otimes\sigma_3),$$
$$(\cos\beta_3\sigma_0\otimes\sigma_0 - i\sin\beta_3\sigma_3\otimes\sigma_1), \quad (18)$$

$$U(\nu_1,\nu_2,\nu_3,\nu_4) = \exp(i\nu_4)M, \text{ where}$$

$$M = \begin{pmatrix} 1 & 0 & 0 & 0 \\ 0 & \cos\frac{\nu_2}{2} & 0 & -\exp i\nu_1 \sin\frac{\nu_2}{2} \\ 0 & 0 & 1 & 0 \\ 0 & \exp i\nu_3 \sin\frac{\nu_2}{2} & 0 & \exp i(\nu_1+\nu_3)\sin\frac{\nu_2}{2} \end{pmatrix}. \quad (19)$$

After applying the unitary operations on ρ_{12}, the transformed state ρ'_{12} (say) is given by [38]

$$\rho'_{1,2} = \Pi_{j=1}^{2} L_j^{(2)} U_{1,2} \Pi_{j=1}^{2} L_j^{(1)} \cdot \rho_{12} \cdot \left(\Pi_{j=1}^{2} L_j^{(1)}\right)^{\dagger} U_{1,2}^{\dagger} \left(\Pi_{j=1}^{2} L_j^{(2)}\right)^{\dagger}, \quad (20)$$

where $(\theta_j^{(i)}, \vec{\eta}_j^{(i)})$ denote the parameters of single-qubit unitary $L_j^{(i)}$ [Eq. (16)] and $U_{1,2}$ denote a two-qubit unitary operation. Let $U_{i,i+1}$ denote a two-qubit operation applied over qubits i and $i+1$. Application of the two-qubit unitary operation on a two-qubit state corresponds to global basis change of the state and is referred to as a nonlocal unitary operation [38]. At this point, noted that, for the purpose of the present analysis, the context will be different. The term "nonlocal unitary operation" will be incompatible. This is because, in the present scenario, such an operation will be applied locally by a single party on its share of two qubits (for details, see Sec. IV).

G. Hamiltonian gate

A Hamiltonian gate $U(H)$ is a unitary gate $\exp(-itH)$ corresponding to time evolution of a quantum system with hermitian Hamiltonian H [34,39]. For both single and two-qubit Hamiltonians H, a Hamiltonian gate can be decomposed into basis gates [39].

H. Imperfect measurements

For all $i = 1, 2, \ldots, n+1$, let party $\mathcal{P}_i$ perform measurements in imperfect devices that fail to detect particles with some probability. For $\mathcal{P}_i$, denoting $M_{i,\bar{o}}^{\text{ideal}}$ as the projector corresponding to output string $\bar{o}$ in ideal qubit projective measurements, the positive operator-valued measure (POVM) elements corresponding to the noisy measurement are given by

$$M_{i,\bar{o}}^{\text{noisy}} = \beta_i M_{i,\bar{o}}^{\text{ideal}} + \frac{1-\beta_i}{2^m}(\mathbb{I}_2)^{\otimes_{k=1}^{m}} \;\forall\, i = 1, 2, \ldots, n+1, \quad (21)$$

where $\beta_i \in [0,1]$ is the noise parameter, and $\bar{o} = (o_1, o_2, \ldots, o_m)$ is the output string of length m. Details of the imperfect measurements to be used in the paper are given in Table III.

TABLE III. Details of the noisy Bell basis, n-qubit GHZ basis, and projective measurements.

Measurement	Noise parameter	POVM elements in Eq. (21)
Bell basis	$\beta_i^{(n)}$	$M_{i,(j_1,j_2)}^{\text{ideal}}$ $j_1, j_2 \in \{0,1\}$ corresponding to four Bell states
n-qubit GHZ basis	$\gamma_i^{(n)}$	$M_{i,(j_1,j_2,\ldots,j_n)}^{\text{ideal}}$ $j_1, j_2, \ldots, j_n \in \{0,1\}$ corresponding to 2^n GHZ states
Projection along arbitrary direction $\vec{s}$	$\delta_i^{(n)}$	$M_{i,(0)}^{\text{ideal}} = \frac{1}{2}(\mathbb{I} + \vec{s}\cdot\vec{\sigma})$ $M_{i,(1)} = \frac{1}{2}(\mathbb{I} - \vec{s}\cdot\vec{\sigma})$

IV. CHARACTERIZING $\mathcal{I}_\mathcal{T}$-TYPE ABSOLUTE n-LOCALITY

A. $\mathcal{I}_\mathcal{T}$-type absolute n-local correlations

Consider an n-local quantum network $\mathcal{N}_\mathcal{T}$ (see Secs. III B and III C). Let $\mathcal{I}_\mathcal{T}$ denote an n-local inequality [Eq. (6)] associated with $\mathcal{N}_\mathcal{T}$. After the sources distribute the particles in the network, let each of the parties perform local unitary operations on their respective subsystems. Each of the extreme parties, receiving single particle, can perform a single-qubit unitary operations [Eq. (16)]. Each of the intermediate parties receiving m ($2 \leqslant m \leqslant n$) can perform both 1-qubit [Eq. (16)] and ($m' \leqslant m$)-qubit unitary operations on the joint state of m qubits received from the sources. The parties then perform local measurements $\mathcal{M}_j (j = 1, 2, \ldots, n+1)$ on their particles (as detailed in Sec. III C). Correlations generated at the end of the measurements are then used to test violation of the correlators based inequality $\mathcal{I}_\mathcal{T}$. It may happen that the correlations fail to violate any n-local inequality associated with the network. This forms the basis of defining the notion of $\mathcal{I}_\mathcal{T}$-type absolute n-locality.

Definition. In $\mathcal{N}_\mathcal{T}$, given an n-local inequality ($\mathcal{I}_\mathcal{T}$), when all the parties perform local unitary operations on their respective subsystems, if the $(n+1)$-partite measurement correlations do not violate $\mathcal{I}_\mathcal{T}$, then such correlations are defined to be $\mathcal{I}_\mathcal{T}$-type absolute n-local correlations and the corresponding nature of such correlations is termed $\mathcal{I}_\mathcal{T}$-type absolute n-locality.

Given any configuration $\mathcal{T}$ and any n-local inequality $\mathcal{I}_\mathcal{T}$, let $\mathcal{A}_{\mathcal{I}_\mathcal{T}}$ denote the set of $\mathcal{I}_\mathcal{T}$-type absolute n-local correlations in $\mathcal{N}_\mathcal{T}$. Clearly, in any $\mathcal{N}_\mathcal{T}$, correlations having n-local models [Eq. (4)] are members of $\mathcal{A}_{\mathcal{I}_\mathcal{T}}$ for any $\mathcal{I}_\mathcal{T}$ associated with $\mathcal{N}_\mathcal{T}$. For example, in an n-local linear network ($\mathcal{N}_{\text{linear}}$), if all the sources generate Werner states [40] with visibility less than or equal to $1/2$, correlations, generated in the network, have an n-local model [9]. Such correlations can never violate any n-local inequality compatible with $\mathcal{N}_{\text{linear}}$. Hence, these correlations belong to $\mathcal{A}_{\mathcal{I}_{\text{linear}}}$ for any n-local inequality $\mathcal{I}_{\text{linear}}$ compatible with $\mathcal{N}_{\text{linear}}$.

Having introduced the notion, the associated mathematical formalism is discussed below.

B. Mathematical formalism

for all $i = 1, 2, \ldots, n$, let source $\mathbf{S}_i$ generate a state $\rho_{i,i+1}$. After distribution of particles from the sources, ρ_{in} (Eq. (7) is the overall state of the network. Each of the parties then perform local unitary operations on its respective share of ρ_{in}. After local basis change applied by the parties, let ρ_f denote the transformed state in the entire network:

$$\rho_f = \left(\otimes_{j=1}^{n+1}\mathcal{U}_j\right)\cdot\rho_{\text{in}}\cdot\left(\otimes_{j=1}^{n+1}\mathcal{U}_j\right)^{\dagger}, \quad (22)$$

where

$$\mathcal{U}_j = \text{1-qubit unitary } L_j \tag{23}$$

[Eq. (16)] if $\mathcal{P}_j$ is an extreme party, and

$$\mathcal{U}_j = \Pi_{k_j} L^{(2)}_{k_j} \cdot U_{m'_j} \cdot \Pi_{k_j} L^{(1)}_{k_j} \tag{24}$$

if $\mathcal{P}_j$ is an intermediate party with $k_j \in \{1, 2, \ldots, 2n\}$ labeling the qubit received by $\mathcal{P}_j$, $L^{(1)}_{k_j}$, $L^{(2)}_{k_j}$ denoting 1-qubit unitaries [Eq. (16)], and m'_j denoting the set of qubits received by $\mathcal{P}_j$ such that over the joint state of these qubits $\mathcal{P}_j$ applies $U_{m'_j}$, where $U_{m'_j}$ denotes $|m'_j|$-qubit unitaries with $|m'_j| \leqslant m$ denoting cardinality of the set m'_j.

Let $\mathcal{C}_{\mathcal{I}_\mathcal{T}}$ denote the collection of correlation terms resulting due to measurements on ρ_f [Eq. (22)]. $\mathcal{C}_{\mathcal{I}_\mathcal{T}}$ is used to test the n-local inequality $\mathcal{I}_\mathcal{T}$. In case, these terms satisfy $\mathcal{I}_\mathcal{T}$ for any possible unitary operations and measurement settings, then $\mathcal{C}_{\mathcal{I}_\mathcal{T}} \in \mathcal{A}_{\mathcal{I}_\mathcal{T}}$. The set of $\mathcal{I}_\mathcal{T}$-type absolute n-local correlations is thus given by

$$\mathcal{A}_{\mathcal{I}_\mathcal{T}} = \left\{ \mathcal{C}_{\mathcal{I}_\mathcal{T}} | \mathcal{C}_{\mathcal{I}_\mathcal{T}} \text{ satisfy } \mathcal{I}_\mathcal{T} \; \forall \, L_j, L^{(1)}_{k_j}, L^{(2)}_{k_j}, U_{m'_j} \right\}. \tag{25}$$

Correlations lying outside $\mathcal{A}_{\mathcal{I}_\mathcal{T}}$ are thus non-n-local. Such types of non-n-local correlations, residing outside $\mathcal{A}_{\mathcal{I}_\mathcal{T}}$, may be referred to as not-$\mathcal{I}_\mathcal{T}$-type absolute n-local correlations.

C. Examples in $\mathcal{N}_{\text{linear}}$ [11]

Consider the n-local inequality given by Eq. (8) in the n-local linear network ($\mathcal{N}_{\text{linear}}$). To date, Eq. (8) is the only existing $\mathcal{I}_{\text{linear}}$. In case only pure product states are involved, correlations generated in $\mathcal{N}_{\text{linear}}$ do not violate $\mathcal{I}_{\text{linear}}$ Eq. (8) even when all parties perform local basis change. The following theorem justifies the claim.

Theorem 1. $\mathcal{I}_{\text{linear}}$-type absolute n-local correlations are generated in $\mathcal{N}_{\text{linear}}$ if each of the sources distributes a two-qubit pure product state when Eq. (8) is considered as the $\mathcal{I}_{\text{linear}}$.

Proof. See Appendix A. ■

D. Examples in a nonlinear network [12]

Consider $\mathcal{N}_{n\text{-star}}$ (Fig. 3). The existing n-local inequality for $\mathcal{N}_{n\text{-star}}$ is given by Eq. (11). Compared with $\mathcal{N}_{\text{linear}}$, similar results hold in $\mathcal{N}_{n\text{-star}}$.

Theorem 2. Considering Eq. (11) as $\mathcal{I}_{n\text{-star}}$, in $\mathcal{N}_{n\text{-star}}$, $\mathcal{I}_{n\text{-star}}$-type absolute n-local correlations are generated when each of the sources distributes a two-qubit pure product state.

Proof: Similar to Theorem 1. ■

E. Utility of characterization

In $\mathcal{N}_\mathcal{T}$, let $\mathcal{B}_\mathcal{T}$ denote the set of all n-local inequalities $\mathcal{I}_\mathcal{T}$ compatible with $\mathcal{N}_\mathcal{T}$. Let Ω denote the set of all two-qubit states. Let us fix an inequality $\mathcal{I}$ from $\mathcal{B}_\mathcal{T}$. Members of Ω can be categorized as follows (see Fig. 4):

(1) For some states, correlations generated in $\mathcal{N}_\mathcal{T}$ admit n-local model [Eqs. (3) and (4)]. Let R_1 denote the corresponding subset of Ω.

(2) Let all the parties perform any possible form of local unitary operations on their respective share of qubit(s). Under such assumption, for some members from Ω, resulting measurement correlations do not violate the n-local inequality $\mathcal{I}$. Let R_2 denote the collection of such states. Clearly, $R_1 \subseteq R_2 \subseteq \Omega$. Correlations generated from the states in R_2 lie in $\mathcal{A}_\mathcal{I}$ [Eq. (25)].

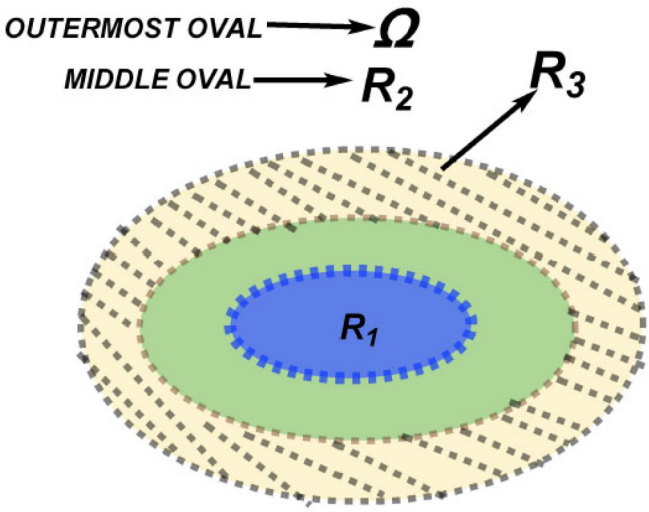

FIG. 4. Categorization of two-qubit state space.

(3) Under the same assumption, violation of $\mathcal{I}$ may be observed for some members of Ω. Clearly $\Omega \setminus R_2 = R_3$ (say) denote the collection of such states. Correlations generated from the members of R_3 are not-$\mathcal{I}$-type absolute n-local correlations.

For states lying in $R_2 \setminus R_1$, violation of $\mathcal{I}$ cannot be observed though corresponding correlations (generated in $\mathcal{N}_\mathcal{T}$) do not admit any n-local hidden variable model and hence are non-n-local. Such states are thus useless. R_3 being a subset of Ω, members from R_3 do not violate $\mathcal{I}$ if the parties are not allowed to perform any unitary operation. Utility of such states in simulating detectable non-n-locality can be exploited only by applying suitable local basis change. The present study thus stresses overanalyzing R_3 because this region clearly points out the efficacy of applying suitable local unitary operations in this context.

V. EFFECTIVENESS OF UNITARIES

For further investigation, the bilocal network ($n = 2$ in Fig. 2) and trilocal network in the star configuration ($n = 3$ in Fig. 3) are considered. Let $\mathcal{N}_{\text{bilocal}}$ and $\mathcal{N}_{3\text{-star}}$ denote the bilocal network and trilocal star network, respectively. These two are the simplest n-local networks of linear and nonlinear types, respectively. The solo motivation of the present study is to explore the utility (if any) of local unitary operations in exploiting non-n-locality both in linear and nonlinear network configurations. So, obvious complexity (for large n) has been avoided by confining to the simplest linear (for $n = 2$) and nonlinear (for $n = 3$) n-local networks. However, few instances of non-4-locality are also provided in $\mathcal{N}_{4\text{-star}}$.

Bilocal inequality [Eq. (8)] and n-local inequality [Eq. (11)] have been considered for $\mathcal{N}_{\text{bilocal}}$ and $\mathcal{N}_{n\text{-star}}$(for $n = 3, 4$), respectively. For the specific measurement contexts (see Sec. III D, Fig. 3), Eqs. (8) and (11) are the only existing n-local inequalities compatible with these two specific networks. The upper bounds [Eqs. (10) and (14)] of each of Eqs. (8) and (11) exist in the literature. As discussed before,

violation of $\mathcal{I}_{\text{bilocal}}$ is observed in $\mathcal{N}_{\text{bilocal}}$ if Eq. (10) is satisfied. Similarly in $\mathcal{N}_{3\text{-star}}$ ($\mathcal{N}_{4\text{-star}}$), violation of $\mathcal{I}_{3\text{-star}}$ ($\mathcal{I}_{4\text{-star}}$) is observed if Eq. (14) [Eq. (15)] is satisfied.

To this end, it must be pointed out that these upper bounds were derived under the assumption that the parties perform suitable single-qubit local unitary operations [Eq. (16)]. In this context, it becomes imperative to explore whether multiqubit unitaries can provide more advantages in simulating detectable nonbilocality and non-n-locality in $\mathcal{N}_{\text{bilocal}}$ and $\mathcal{N}_{n\text{-star}}$, respectively. Affirmative findings are discussed next.

A. Instances of not-$\mathcal{I}_{\text{bilocal}}$-type absolute bilocality

1. Strategy for detection

Let two states $\rho_{1,2}$, $\rho_{2,3}$ used in $\mathcal{N}_{\text{bilocal}}$ be such that Eq. (10) is violated. This implies that violation of $\mathcal{I}_{\text{bilocal}}$ is not possible even if the parties are allowed to perform only single-qubit unitary operations. Such an observation consequently points out the impossibility of violation of $\mathcal{I}_{\text{bilocal}}$ when the parties do not perform any local unitary operations. Now, let the parties perform any possible form of local unitary operations. Under such an assumption, if the resulting tripartite measurement correlations violate $\mathcal{I}_{\text{bilocal}}$ [Eq. (10)], then $\rho_{1,2}$, $\rho_{2,3}$ have generated not-$\mathcal{I}_{\text{bilocal}}$-type absolute bilocality.

Equation (10) is satisfied if both $\mathcal{S}_1$, $\mathcal{S}_2$ distribute pure entangled states in $\mathcal{N}_{\text{bilocal}}$ [17]. However, in case one of the sources distribute a mixed entangled state, no definite conclusion exists. $\mathcal{N}_{\text{bilocal}}$, where one or both the sources distribute mixed two-qubit entangled state(s), is thus considered next.

2. One source generating a mixed entangled state

Let $\mathcal{S}_1$ send a pure entangled state [34]

$$\rho_{1,2} = (\sin\mu_1|01\rangle + \cos\mu_1|10\rangle)(\sin\mu_1\langle 01| + \cos\mu_1\langle 10|), \tag{26}$$

with $\mu_1 \in (0, \pi/2)$. Let the other source distribute states from the following class of mixed entangled state [41,42]:

$$\rho_{2,3} = \omega_2|00\rangle\langle 00| + (1-\omega_2)(\sin\alpha_2|01\rangle + \cos\alpha_2|10\rangle)(\sin\alpha_2\langle 01| + \cos\alpha_2\langle 10|), \tag{27}$$

with $\omega_2 \in [0, 1]$ and $\alpha_2 \in [0, \frac{\pi}{4}]$. There exist members from these two families [Eqs. (26) and (27)] for which violation of $\mathcal{I}_{\text{bilocal}}$ is observed if $\mathcal{P}_2$ applies suitable single-qubit [Eq. (16)] and two-qubit unitaries [Eq. (17)] on its share of two qubits [see Fig. 5(a)]. Details of a particular instance of such violation are given in the second row of Table IV.

3. Both sources generating mixed entangled states

For $i = 1, 2$, let $\mathcal{S}_i$ distribute a state from the above class of mixed entangled states [Eq. (27), for parameters $\omega_1, \omega_2, \alpha_1, \alpha_2$]. For some members from these classes of states [Eq. (27)], the upper bound of Eq. (8) is $\leqslant 1$. But for suitable local unitary operation [Eq. (19)] applied by the intermediate party, violation of $\mathcal{I}_{\text{bilocal}}$ is observed [see Fig. 5(b)]. A particular instance of not-$\mathcal{I}_{\text{bilocal}}$-type absolute bilocality is detailed in the third row of Table IV.

Instances of violation discussed so far occur in the network when both sources generate entangled two-qubit states. In this context, an obvious query arises: in the presence of suitable local unitaries, can nonbilocality be detected if one of the sources distributes a product state? The following theorem provides a negative response to this query.

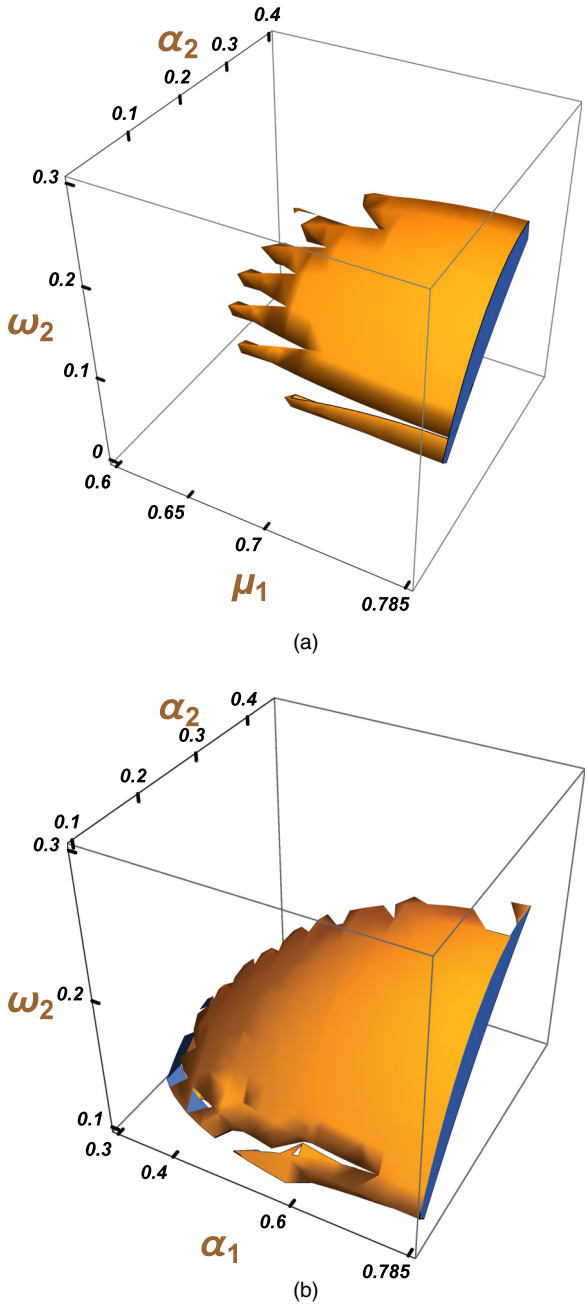

FIG. 5. Shaded region in both panels give the range of state parameters for which not absolute $\mathcal{I}_{\text{bilocal}}$-type bilocal correlations are simulated. Details of the local unitary operations applied by $\mathcal{P}_2$ corresponding to panels (a) and (b) are provided in the second and third rows of Table IV, respectively. Panel (a) gives the range of state parameters when only one pure entangled state is used in $\mathcal{N}_{\text{bilocal}}$. Panel (b) shows the corresponding range of parameters for two mixed entangled states [Eq. (27)] with $\omega_1 = 0.005$. It may be noted that none of these states satisfy the relation given by Eq. (10).

Theorem 3. $\mathcal{I}_{\text{bilocal}}$-type absolute correlations are generated in $\mathcal{N}_{\text{bilocal}}$ if at least one of the sources distributes a two-qubit pure product state.

TABLE IV. Details of violation instances of $\mathcal{I}_{\text{bilocal}}$ [Eq. (8)], $\mathcal{I}_{\text{3-star}}$, and $\mathcal{I}_{\text{4-star}}$ [Eq. (11)] are enlisted here. Second and third rows contain details related to $\mathcal{N}_{\text{bilocal}}$ while the remaining rows correspond to that in $\mathcal{N}_{\text{3-star}}$ and $\mathcal{N}_{\text{4-star}}$ Here, in all these networks, only the intermediate party ($\mathcal{P}_2$ in $\mathcal{N}_{\text{bilocal}}$ and $\mathcal{P}_1$ in $\mathcal{N}_{\text{3-star}}$ and $\mathcal{N}_{\text{4-star}}$) performs local unitary operations. Details of all the nonidentity unitary operations are given in the second and third columns. The states considered here cannot show the violation of $\mathcal{I}_{\text{bilocal}}$ [Eq. (8)] or $\mathcal{I}_{n\text{-star}}$ [Eq. (11)] for $n = 3, 4$) if none of the parties are allowed to perform any local unitary operation. As discussed in Sec. V A, this fact is implied by fourth column of the table.

State parameters	1-qubit unitary Eq. (16)	2-qubit unitary	L.H.S. value of Eq. (10) or Eq. (14) or Eq. (15)	L.H.S. value of Eq. (8) or Eq. (11)
$\mu_1 = \pi/4$ in Eq. (26) and $(\alpha_2, \omega_2) = (0.152, 0.13)$ in Eq. (27)	$(\theta_{2,2}^{(2)}, \theta_{2,3}^{(2)}) = (-1.05316, -0.00039)$ $\vec{\eta}_2^{(2)} = (-0.99220, 0.12067, -0.013127)$ $\vec{\eta}_3^{(2)} = (-0.92711, 0.19909, 0.31754)$	$(\phi_1, \phi_2, \phi_3) =$ $(-0.03753, 0, -1.40698)$ in Eq. (17)	0.99996 in Eq. (10)	1.02142 in Eq. (8)
$(\alpha_1, \omega_1) = (0.6, 0.005)$, $(\alpha_2, \omega_2) = (0.24, 0.175)$ in Eq. (27)		$(\nu_1, \nu_2, \nu_3, \nu_4) =$ $(2, 0.50001, 0.90421, 0)$ in Eq. (19)	0.99840 in Eq. (10)	1.01677 in Eq. (8)
$(\mu_1, \mu_3) = (\pi/4, \pi/4)$ in Eq. (26)		$(\beta_1, \beta_2, \beta_3) = (\pi/2, \pi/2, 0)$ in Eq. (18)	2 in Eq. (14)	2.24492 in Eq. (11) for $n = 3$
$(\upsilon_1, \upsilon_3) = (0.89, 0.87)$ in Eq. (29)		$(\beta_1, \beta_2, \beta_3) = (\pi/2, \pi/2, 0)$ in Eq. (18)	2 in Eq. (14)	2.06144 in Eq. (11) for $n = 3$
$(\alpha_1, \omega_1) = (0.785, 0.1)$, $(\alpha_2, \omega_2) = (0.053176, 0.07)$ $(\alpha_3, \omega_3) = (0.785, 0.07)$ in Eq. (27)		$(\nu_1, \nu_2, \nu_3, \nu_4) =$ $(2.90996, 1.28896, -0.281838, 0)$ in Eq. (19)	1.99288 in Eq. (14)	2.01637 in Eq. (11) for $n = 3$
$(\mu_1, \mu_3, \mu_4) = (\pi/4, \pi/4, \pi/4)$ in Eq. (26)		$(\beta_1, \beta_2, \beta_3) = (\pi/2, \pi/2, 0)$ in Eq. (18)	4 in Eq. (15)	4.75863 in Eq. (11) for $n = 4$
$(\epsilon_1, \epsilon_2, \epsilon_3) =$ $(0.99, 0.0029, 0.99)$ $\delta_1 = \delta_2 = \delta_3 = 0.99$ in Eq. (31)		$(\nu_1, \nu_2, \nu_3, \nu_4) =$ (1.84378,3.14,0.27298,0) in Eq. (19)	1.9998 in Eq. (14)	2.2076 in Eq. (11) for $n = 3$
$\gamma_1 = \gamma_5 = 0.1$, $\gamma_3 in [0, 1]$ $\mu_1 = \mu_3 = \pi/4$, $\mu_2 = 0$ in Eq. (32)		$(\nu_1, \nu_2, \nu_3, \nu_4) =$ $(0.7448, -0.2231, -3.14, 0)$ in Eq. (19)	2 in Eq. (14)	2.0926 in Eq. (11) for $n = 3$
$(\gamma_1, \gamma_5, \gamma_7) =$ $(0.01, 0.05, 0.1)$, $\gamma_3 \in [0, 1]$ $\mu_1 = \mu_3 = \mu_4 = \pi/4$, $\mu_2 = 0$ in Eq. (32)		$(\nu_1, \nu_2, \nu_3, \nu_4) =$ $(-0.7070, 0.9344, -3.14, 0)$ in Eq. (19)	4 in Eq. (15)	5.426 in Eq. (11) for $n = 4$

Proof. If both $\rho_{1,2}$ and $\rho_{2,3}$ are pure product states then this theorem is same as Theorem 1 for $n = 2$.

If a single two-qubit pure product state is involved in $\mathcal{N}_{\text{bilocal}}$, the proof of this theorem is given in Appendix B.

Theorem 3 thus prescribes an entanglement detection criterion in $\mathcal{N}_{\text{bilocal}}$ provided the network only involves pure two-qubit states.

In $\mathcal{N}_{\text{3-star}}$, $\mathcal{N}_{\text{4-star}}$, a contrasting result is observed. There, non-n-locality ($n = 3, 4$) can be detected involving a two-qubit pure product state when $\mathcal{P}_1$ performs suitable two-qubit unitary operations on the joint state of its three qubits. Violation of $\mathcal{I}_{n\text{-star}}$ [Eq. (11) for $n = 3, 4$] in presence of local unitary operations are discussed next. ■

B. Instances of not-$\mathcal{I}_{n\text{-star}}$-type absolute trilocality for $n = 3, 4$

1. Detection strategy

A strategy similar to that followed for $\mathcal{N}_{\text{bilocal}}$ will be adopted here. Let $\mathcal{S}_i$ distribute a two-qubit state $\rho_{i,i+1}$ $(i = 1, 2, 3)$ such that corresponding correlations violate the relation given by Eq. (14). Now, when all the parties are allowed to perform local unitary operations, if resulting measurement correlations violate $\mathcal{I}_{3\text{-star}}$ [Eq. (11), $n = 3$], then $\rho_{1,2}$, $\rho_{2,3}$, $\rho_{3,4}$ have generated not-$\mathcal{I}_{n\text{-star}}$-type absolute trilocality. Similarly, in $\mathcal{N}_{4\text{-star}}$, if violation of $\mathcal{I}_{4\text{-star}}$ [Eq. (11), $n = 4$] is observed then $\rho_{i,i+1}$ $(i = 1, 2, 3, 4)$ have generated not-$\mathcal{I}_{4\text{-star}}$-type absolute 4-locality.

2. $\mathcal{N}_{3\text{-star}}$ involving two entangled and one pure product state

First, let each of $\mathcal{S}_1, \mathcal{S}_3$ distribute a pure entangled state [Eq. (26) with parameters μ_1, μ_3 for $\rho_{1,2}$ and $\rho_{3,4}$, respectively], Let $\mathcal{S}_2$ generate a two-qubit pure product state:

$$\rho_{2,3} = \frac{1}{4} \sum_{i,j,k,l=0}^{1} |ij\rangle\langle kl|. \tag{28}$$

Let $\mathcal{P}_1$ perform two-qubit unitary operation of the form given by Eq. (18). There exist members from these families of states [Eqs. (26) and (28)] for which four-partite correlations generated in $\mathcal{N}_{3\text{-star}}$ fall outside $\mathcal{A}_{\mathcal{I}_{3\text{-star}}}$ [Fig. 6(a)].

Next, let each of $\mathcal{S}_1, \mathcal{S}_3$ generate states from the Werner family of two-qubit mixed entangled states [40]:

$$\rho_{i,i+1} = \frac{(1 - v_i)}{4} \mathbb{I}_{2\times 2} + v_i[|01\rangle\langle 01| + |10\rangle\langle 10| - (|01\rangle\langle 10| + |10\rangle\langle 01|)], \quad v_i \in [0, 1), \quad i = 1, 3. \tag{29}$$

Let $\mathcal{S}_2$ distribute a pure product state [Eq. (28)]. Over some range of noise parameters v_1, v_3 [Fig. 6(b)], violation of $\mathcal{I}_{3\text{-star}}$ [Eq. (11)] is observed when $\mathcal{P}_1$ perform suitable two-qubit unitary operation [Eq. (18)]. Particular instances of violation for both these cases (pure and mixed entanglement), are enlisted in the fourth and fifth rows of Table IV.

3. $\mathcal{N}_{4\text{-star}}$ involving three entangled and one pure product state

Let each of $\mathcal{S}_i (i = 1, 3, 4)$ distribute the maximally entangled state [Eq.] for $\mu_1 = \mu_2 = \mu_4 = \pi/4$ with $\mathcal{S}_3$ generating a two-qubit pure product state [Eq. (28)]. Let $\mathcal{P}_1$ perform a two-qubit unitary operation of the form given by Eq. (18). Violation of 4-local inequality [Eq. (11), $n = 4$] is observed (see seventh row of Table IV).

4. $\mathcal{N}_{3\text{-star}}$ involving only mixed entanglement

For all $i = 1, 2, 3$, let $\rho_{i,i+1}$ be a state from the class of mixed entangled states given by Eq. (27) with state parameters ω_i, α_i. Let the intermediate party $\mathcal{P}_1$ perform the unitary operation given by Eq. (19).

For some members from this family [Eq. (27)], correlations generated fall outside the set $\mathcal{A}_{\mathcal{I}_{3\text{-star}}}$ (Fig. 7). One such example is given in the sixth row of Table IV.

VI. RESISTANCE TO NOISE

An n-local quantum network is compatible with any entanglement distribution protocol. In an ideal situation, any such protocol is supposed to use pure entanglement only. However, due to the unavoidable interaction of the quantum states with the environment, noisy entangled states are involved in such protocols. From a practical viewpoint, it thus becomes important to analyze whether the application of suitable local unitaries can enhance the visibility of noisy quantum states to simulate non-n-locality in any such network scenarios. Two potent factors of noise are considered for further analysis.

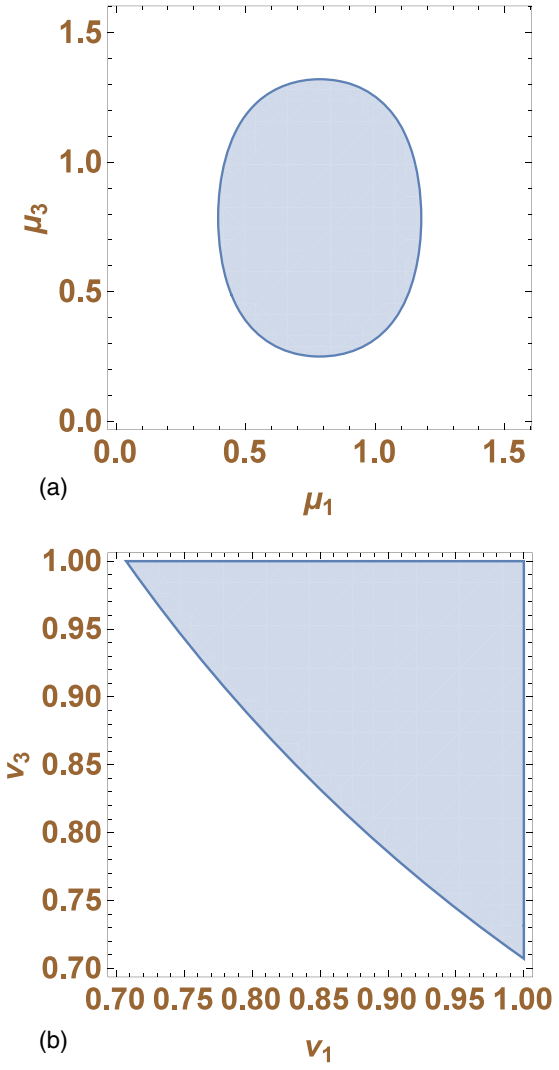

FIG. 6. Shaded region is a subspace of the parameter space for entangled states (Eq. (26)] and Werner class of states [Eq. (29)] in panels (a) and (b), respectively. In panel (a), corresponding to any point from the shaded region, the entangled states used in $\mathcal{N}_{3\text{-star}}$ [involving a pure product state (28)] can generate not-$\mathcal{I}_{3\text{-star}}$-type absolute trilocality. Same is the case in panel (b) with now two states considered from the Werner family [Eq. (29)] along with the pure product state [Eq. (28)]. Details of the local unitary operations applied by $\mathcal{P}_1$ corresponding to panels (a) and (b) are provided in the fourth and fifth rows of Table IV, respectively. None of these states satisfy the relation given by Eq. (14) if the parties do not perform any local basis change.

A. Noisy entanglement generation

In an ideal $\mathcal{N}_{3\text{-star}}$, initially, let each of the three sources have the state $\rho = |01\rangle\langle 01|$. The Bell state $|\phi^-\rangle\langle\phi^-|$ is cre-

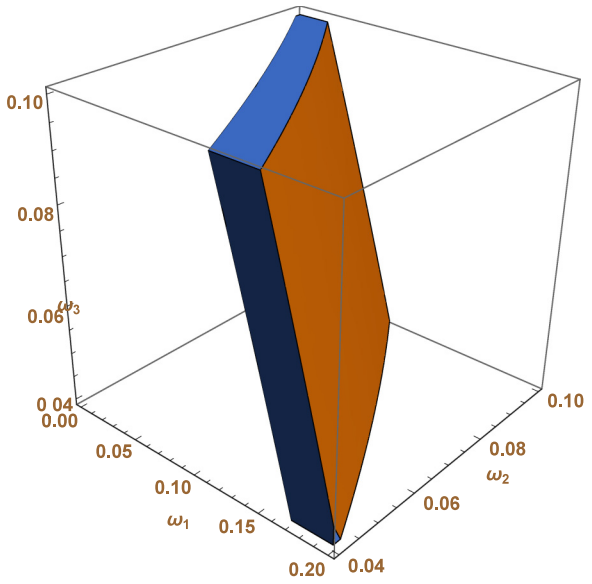

FIG. 7. Shaded region specify members from a family of mixed entangled states [Eq. (27)] with $(\alpha_1, \alpha_2, \alpha_3) = (0.785, 0.053176, 0.785)$. Not-absolute $\mathcal{I}_{3\text{-star}}$-type trilocal correlations are generated when these members are used in $\mathcal{N}_{3\text{-star}}$. Details of the local unitary operations involved are provided in the sixth row of Table IV. None of these states satisfy the relation given by Eq. (10).

ated [6] by applying the Hadamard gate $\mathcal{H}$ on the first qubit followed by the CNOT ($\mathcal{CNOT}$) gate (considering first qubit as control qubit). In practical situations, owing to imperfections in both one and two-qubits operations, noisy entanglement is generated. At each source, let ϵ and δ denote the parameters characterizing imperfections in $\mathcal{H}$ and $\mathcal{CNOT}$, respectively. State (ρ') resulting from the application of a noisy Hadamard gate is given by [43]

$$\rho' = \epsilon\big(\mathcal{H} \otimes \mathbb{I}_2 \cdot \rho \cdot \mathcal{H}^\dagger \otimes \mathbb{I}_2\big) + \frac{1-\epsilon}{2}\mathbb{I}_2 \otimes \rho_2,$$

where $\rho_2 = \mathrm{Tr}_1(\rho)$.

$$= \frac{1}{2}(|00\rangle\langle 00| + |10\rangle\langle 10|) - \frac{\epsilon}{2}(|00\rangle\langle 10| + |10\rangle\langle 00|). \quad (30)$$

After applying the noisy $\mathcal{CNOT}$, ρ' becomes [43]

$$\rho'' = \delta\big(\mathcal{CNOT} \cdot \rho' \cdot (\mathcal{CNOT})^\dagger\big) + \frac{1-\delta}{4}\mathbb{I}_2 \otimes \mathbb{I}_2$$

$$= \frac{1}{4}\Bigg[\sum_{i,j=0}^{1}(1 + (-1)^{i+j}\delta)|ij\rangle\langle ij|$$

$$- 2\epsilon\delta(|11\rangle\langle 00| + |00\rangle\langle 11|)\Bigg]. \quad (31)$$

In realistic situations, for all i, let $\mathcal{S}_i$ distribute ρ_i'' [Eq. (31) with parameters ϵ_i, δ_i] in $\mathcal{N}_{3\text{-star}}$. On receiving the qubits, let $\mathcal{P}_1$ perform two-qubits local unitary operations [Eq. (19)]. Corresponding correlations are then used to test $\mathcal{I}_{3\text{-star}}$ [Eq. (11)]. For $(\nu_1, \nu_2, \nu_3, \nu_4) = (1.84378, 3.14, 0.27298, 0)$ in Eq. (19) and $\epsilon_3 = \epsilon_1$ and $\delta_3 = \delta_2 = \delta_1$ in Eq. (31), there exist ranges of noise parameters $(\epsilon_1, \epsilon_2, \delta_1)$ for which violation of Eq. (11) is observed [see Fig. 8(a)]. For such a range of noise parameters, violation of $\mathcal{I}_{3\text{-star}}$ is not possible if none of the parties is allowed to perform any local unitary operation in $\mathcal{N}_{3\text{-star}}$. A numerical instance is given in the eighth row of Table IV.

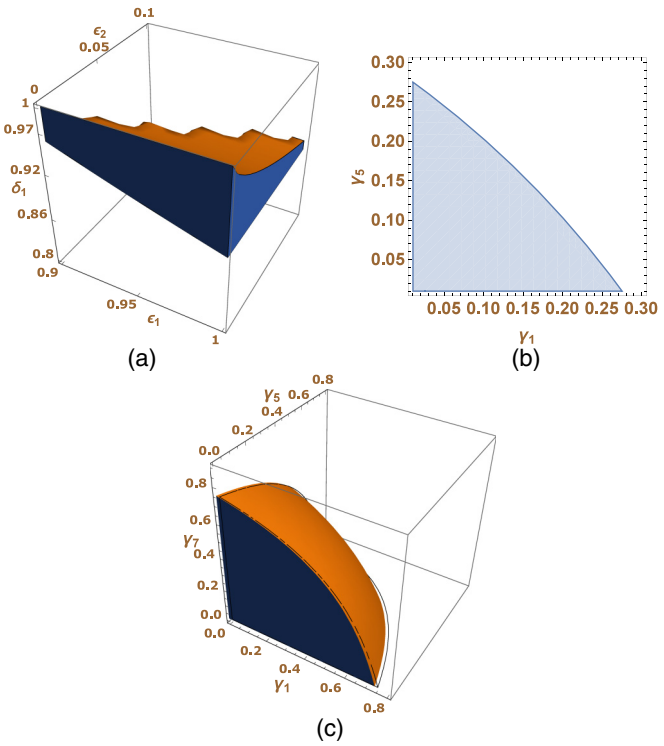

FIG. 8. All panels give region of noise parameters for which violation of n-local inequality is obtained when $\mathcal{P}_1$ apply suitable two-qubit local basis change given by Eq. (19) on the joint state of its qubits in (a) $\mathcal{N}_{3\text{-star}}$ and (b), (c) $\mathcal{N}_{4\text{-star}}$. In panel (a) noisy states resulting from erroneous entanglement generation are considered. Panels (b) and (c) involve states resulting from communication of both qubits of $\rho_{i,i+1}$ through phase-damping channel Γ_i in $\mathcal{N}_{3\text{-star}}$ and $\mathcal{N}_{4\text{-star}}$, respectively. Specifications of the phase-damped noisy states $\rho'_{i,i+1}$ [Eq. (32)] are as follows: (b) $(\mu_1, \mu_2, \mu_3) = (\pi/4, 0, \pi/4)$, (c) $(\mu_1, \mu_2, \mu_3, \mu_4) = (\pi/4, 0, \pi/4, \pi/4)$ with $\gamma_3 \in [0, 1]$ in both panels (b) and (c). States corresponding to any of the shaded regions indicate higher tolerance against noise obtained when $\mathcal{P}_1$ applies suitable two-qubit unitary operation. So violation of Eq. (11) is not observed when any of these noisy states are used in the usual (a), (b) $\mathcal{N}_{3\text{-star}}$ and (c) $\mathcal{N}_{4\text{-star}}$, where the parties either do not apply any local basis change or perform at most single-qubit local unitary operations prior to measurements. Details of the two-qubit unitary operation involved in panels (a)–(c) are specified in the eighth, ninth, and tenth rows of Table IV, respectively.

B. Noisy communication over quantum channels

Let each source generate a pure entangled state in $\mathcal{N}_\mathcal{T}$. Let qubits from at least one of the sources are communicated over noisy quantum channel. Corresponding parties thus receive one or more noisy qubits. In such a situation, there may exist correlations lying outside $\mathcal{A}_{\mathcal{I}_\mathcal{T}}$.

Consider the class of mixed entangled states given by Eq. (27). Such states, up to local unitary transformations, are equivalent to amplitude damped version of pure entan-

gled states. Discussion in Sec. V A clearly points out that, compared with usual $\mathcal{N}_{\text{bilocal}}$ (parties not applying any unitary operation), violation of $\mathcal{I}_{\text{bilocal}}$ is obtained for larger ranges of noise (ω_1, ω_2) [see Fig. 5(b)] when $\mathcal{P}_2$ performs a suitable unitary operation on the joint state of the noisy qubits. Similar findings were discussed in Sec. V B when all the states from this family of mixed entangled states were used in $\mathcal{N}_{3\text{-star}}$ (Fig. 7).

Let $\mathcal{S}_i$ generate a state $\rho_{i,i+1}$ from the family of pure entangled states [Eq. (26)]. For all $i = 1, 2, 3$, let both the qubits of $\rho_{i,i+1}$ be passed through a phase damping channel Γ_i. The phase damped state $\rho'_{i,i+1}$ takes the form [34]

$$\rho'_{i,i+1} = \sin^2\mu_i|01\rangle\langle 01| + \cos^2\mu_i|10\rangle\langle 10| + (1-\gamma_i) \times \cos\mu_i \sin\mu_i(|01\rangle\langle 10| + |10\rangle\langle 01|) \quad \text{with } i = 1, 2, 3. \tag{32}$$

γ_i denotes the probability with which phase damping occurs when a qubit is passed through Γ_i. Let $\gamma_2 = \gamma_1$, $\gamma_4 = \gamma_3$, and $\gamma_6 = \gamma_5$. Consider specific pure states [Eq. (26)] given by $(\mu_1, \mu_2, \mu_3) = (\pi/4, 0, \pi/4)$. It may be noted that, for $\mu_2 = 0$, $\rho_{2,3}$ is a pure product state. When phase damped versions of these specific states are used in $\mathcal{N}_3$ and each of the parties perform single-qubit unitary operations, then corresponding correlations do not violate $\mathcal{I}_{3\text{-star}}$ because the left-hand side (L.H.S.) of Eq. (14) turns out to be two. Similarly, no violation of $\mathcal{I}_{4\text{-star}}$ [L.H.S. of Eq. (15) gives four] is obtained in $\mathcal{N}_{4\text{-star}}$ involving these three particular states and $\rho'_{4,5}$ with $\mu_4 = \frac{\pi}{4}$.

Now, let us consider the case when the intermediate party $\mathcal{P}_1$ performs two-qubit unitary operation given by Eq. (19). Non-n-local correlations are simulated over some range of noise parameters [see Figs. 8(b) and 8(c)]. Thus, in $\mathcal{N}_{n\text{-star}}(n = 3, 4)$, involving two-qubit unitary operations (by $\mathcal{P}_1$), $\mathcal{I}_{n\text{-star}}$ offers more resistance to phase damping noise. A specific instance of such unitary operations [Eq. (19)] in each $\mathcal{N}_{3\text{-star}}$ and $\mathcal{N}_{4\text{-star}}$ is given in the ninth and tenth row of Table IV, respectively.

C. Error due to imperfection in measurements

In contrast with ideal measurement contexts, the devices used by the parties may be imperfect in the sense that any such device may fail to detect the outputs with some nonzero probability (see Sec. III H). This in turn leads to generation of noisy correlation statistics, the source of error being the failure probability of output detection. To exploit the utility of unitary operations in offering more resistance to such type of noise, $\mathcal{N}_{\text{linear}}$ and $\mathcal{N}_{n\text{-star}}$ are considered.

In $\mathcal{N}_{\text{linear}}$ ($\mathcal{N}_{n\text{-star}}$) let each of the intermediate parties (central party) perform imperfect Bell basis (n-qubit GHZ basis) measurement whereas each of the extreme parties (in both the networks) perform noisy projective measurement [see Eq. (21) and Table III]. Resulting measurement statistics are then used to test violation of corresponding n-local inequality: Eq. (8) in $\mathcal{N}_{\text{linear}}$ and Eq. (11) in $\mathcal{N}_{n\text{-star}}$.

Theorem 4. If V_{linear} and $V_{n\text{-star}}$ denote the value of the L.H.S. of n-local inequality, Eqs. (8) and (11), respectively, in an ideal measurement scenario (perfect-measurement context), then violation of Eqs. (8) and (11) is possible in the imperfect-measurement context when Eqs. (33) and (34) hold, respectively,

$$V_{\text{linear}} > \frac{1}{\sqrt{\delta_1^{(\text{noise})}\delta_{n+1}^{(\text{noise})}\prod_{i=2}^{n}\beta_i^{(\text{noise})}}}, \tag{33}$$

$$V_{n\text{-star}} > \frac{2^{n-2}}{\left(\gamma_1^{(\text{noise})}\prod_{i=2}^{n+1}\delta_i^{(\text{noise})}\right)^{\frac{1}{n}}}. \tag{34}$$

Proof. See Appendix C. ■

Considering $\mathcal{N}_{\text{linear}}$, for the sake of simplicity of notation, let V_1 denote the value of the L.H.S. of Eq. (8) or (11) when the parties perform only a single-qubit basis change on their respective share of qubits. Similarly, let V_2 denote the value of the L.H.S. of Eq. (8) or (11) when every party is allowed to perform any possible form of local unitary operation. The application of multiqubit unitary operations helps to generate more-noise-resistant correlations in $\mathcal{N}_{\text{linear}}$ and $\mathcal{N}_{n\text{-star}}$ if Eqs. (35) and (36) hold, respectively:

$$\frac{1}{V_2} < \sqrt{\delta_1^{(\text{noise})}\delta_{n+1}^{(\text{noise})}\prod_{i=2}^{n}\beta_i^{(\text{noise})}} < \frac{1}{V_1}, \tag{35}$$

$$\frac{1}{V_2} < \left(\gamma_1^{(\text{noise})}\prod_{i=2}^{n+1}\delta_i^{(\text{noise})}\right)^{\frac{1}{n}} < \frac{1}{V_1}. \tag{36}$$

The above relations clearly point out that multiqubit unitary operations are effective if $V_1 < V_2$. Several such instances have been discussed in previous sections. For a particular example in $\mathcal{N}_{\text{bilocal}}$, considering the second row of Table IV in a consistent imperfect measurement context, i.e., where all the noise parameters are same: $\delta_1 = \delta_3 = \beta_2 = \beta$ (say). Up to the application of single-qubit unitary operations, violation of Eq. (8) in the presence of consistent imperfection in measurements requires:

$$\beta > \frac{1}{0.99996^{\frac{2}{3}}}. \tag{37}$$

So, violation of Eq. (8) (for $n = 2$) is impossible if the parties use imperfect measurement devices. However, when the parties perform the specific two-qubit unitary operations (detailed in the second row of Table IV), the violation of the inequality is observed for $\beta > 1/1.02142^{\frac{2}{3}} \approx 0.986$.

Similarly for the example of noise resistance offered by 2-qubit unitaries in $\mathcal{N}_{3\text{-star}}$, consider the fourth row in the same Table. If the parties apply only single-qubit unitaries and then measure in imperfect devices with $\delta_2 = \delta_3 = \delta_4 = \gamma_1 = \gamma$ (say), no violation of Eq. (11) is obtained for any $\gamma \in [0, 1)$. If unitary operations, as specified in the fourth row of Table IV, are applied followed by measurement in the imperfect devices, violation of Eq. (11) (for $n = 3$) is observed for any $\gamma \in (0.917, 1]$.

D. Imperfection in unitary operations

For some $j = 1, 2, \ldots, n+1$, let U_j denote an m-qubit ($m \geqslant 1$) local basis change applied by party $\mathcal{P}_j$ on its share of the overall quantum state ρ (say) in the network. Let the unitary operation U_j be imperfect in the sense that there exists a nonzero probability $1 - \lambda^{(\text{noise})}$ (say) with which U_j fails to act. Due to such imperfection in basis change,

ρ evolves to ρ' (say):

$$\rho' = \lambda^{(\text{noise})} U_j \cdot \rho \cdot U_j^\dagger + \left(1 - \lambda^{(\text{noise})}\right)\rho. \tag{38}$$

Such ρ', on being subjected to perfect measurement contexts, may generate non-n-local correlations in corresponding quantum networks over some range of $\lambda^{(\text{noise})}$. For further numerical illustration, let us consider some of the unitary operations from Table IV.

In $\mathcal{N}_{\text{bilocal}}$, let us consider the numerical instance provided in the third row of the table. If $\mathcal{P}_2$ applies the noisy version of the unitary operation over its share of the two specific states mentioned there (third row), nonbilocal correlations are generated for $\lambda^{(\text{noise})} \in [0.91, 1]$. For $\mathcal{N}_{3\text{-star}}$, let us consider the imperfect version of the unitary operation and the particulars of the quantum states mentioned in the fourth row of Table IV. Nontrilocal correlations are observed for any value of $\lambda^{(\text{noise})}$ in the range [0.635,1].

VII. COMPARISON WITH EXISTING n-LOCAL NETWORKS

Since its inception, the source-independence assumption has helped reduce requirements for demonstrating quantum nonlocality compared with the standard Bell scenario. Over years, this assumption has been used in multifaceted applications exploiting quantum nonlocality. As a consequence, several n-local network configurations have emerged.

Keeping pace with such progress, an attempt has been made here to showcase the applicability of suitable 2-qubit unitary operations for simulating nonlocal quantum correlations in such networks. From what has been discussed so far, it can safely be concluded that there exist many such unitary operations, which when applied prior to measurements enhance detection of non-n-local correlations compared with detection of the same in existing network scenarios. Each instance of violation of an n-local inequality (for $n = 2, 3, 4$) provided above takes place in the new network scenario where the parties perform suitable basis change prior to measurements. As has been mentioned each time after providing examples of violation, n-local bounds existing in the literature fail to detect violation of corresponding n-local inequalities for the same quantum states and the same collection of measurement settings. At this point, it may be recalled from earlier discussions that all such bounds were derived in corresponding n-local networks in the absence of multiqubit unitary operations. Hence, such failure of existing n-local bounds, in contrast with observable violation in the new network scenario (involving application of two-qubit basis changes over multiple qubits) clearly imply the effectiveness of multiqubit unitary operations. The last two columns of Table IV reflect the numerics in support of the comparison.

To this end, it may once again be mentioned that such an advantage offered by multiqubit unitaries is indicated by existing results of effectiveness of global unitary operations in exploiting several notions of quantumness (see Sec. I) in standard measurement scenarios involving single sources of quantum states. However, owing to the inherent unphysicalness of applying a global basis change in any such scenario (see Secs. I and II for details), all such results merely reduce to mathematical studies with no proper insight in view of practical situations. But the present study does not suffer from any such drawback because, in network configuration, at least one of the parties get access to multiple qubits and can perform multiqubit unitaries.

TABLE V. Details of the Hamiltonian gates [34] corresponding to 1-qubit [Eq. (16)] and 2-qubit unitary operations (17) and (18) are enlisted here.

Unitary operation	Gates
1-qubit unitary [Eq. (16)]	$\exp^{(-i\frac{\theta}{2}H)}$ with $H = \vec{\eta}\cdot\vec{\sigma}$
2-qubits unitary [Eq. (17)]	$\Pi_{j=1}^{3}\exp^{(-i\phi_j H_j)}$ with $H_j = \sigma_j \otimes \sigma_j,\ j = 1, 2, 3$
2-qubits unitary [Eq. (18)]	$\Pi_{j=1}^{3}\exp^{(-i\beta_j H_j)}$ with $H_1 = \sigma_1 \otimes \sigma_2, H_2 = \sigma_2 \otimes \sigma_3$, $H_3 = \sigma_3 \otimes \sigma_1$

VIII. CIRCUIT IMPLEMENTATION

A unitary operation, applied to any quantum system, is a linear transformation which preserves the norm of the vector representing the state of the system [34]. In quantum information theory, any unitary operation thus corresponds to a reversible operation that does not cause any information loss. Now, quantum gates can be considered as the building blocks of quantum circuits, which are the basic structures used to perform quantum computations. Any unitary operation can be implemented in a quantum circuit using quantum gates.

Consider the single-qubit unitary operation [Eq. (16)]. The quantum gate associated with this unitary transformation is the single-qubit Hamiltonian gate (see Table V). The effect of each of the two 2-qubit unitary operations given by Eqs. (17) and (18) can be obtained by applying a sequence of three 2-qubit Hamiltonian gates (see Table V).

The unitary operation given by Eq. (19) corresponds to a 2-qubits controlled unitary gate $C_R(\nu_1, \nu_2, \nu_3, \nu_4)$ with control on the first qubit and a possible global phase factor $\exp(i\nu_4)$ of the generic single-qubit unitary gate $R(\nu_1, \nu_2, \nu_3)$ that takes $|0\rangle$ to the state $\exp(i\nu_3)[\cos\frac{\nu_1}{2}|0\rangle + \sin\frac{\nu_1}{2}\exp(i\nu_2)|1\rangle]$ [39]. Circuit diagrams [39] for quantum gates corresponding to some of the unitary operations used in Sec. V, i.e., associated with some of the unitary operations enlisted in Table IV, are given in Fig. 9.

IX. DISCUSSION

The notion of non $\mathcal{I}_\mathcal{T}$-type absolute n-locality has been introduced so as to provide a general framework for analyzing the role of multiqubit unitary operations in any given quantum network $\mathcal{N}_\mathcal{T}$. To point out the existence of non-$\mathcal{I}_\mathcal{T}$-type absolute n-local correlations, explicit examples of two-qubit unitary operations enhancing violation of bilocal inequality in linear network and n-local ($n = 3, 4$) inequality in the star network have been provided. As mentioned in Sec. IV, the bounds of n-local inequalities in $\mathcal{N}_{\text{linear}}$ and $\mathcal{N}_{n\text{-star}}$ exist

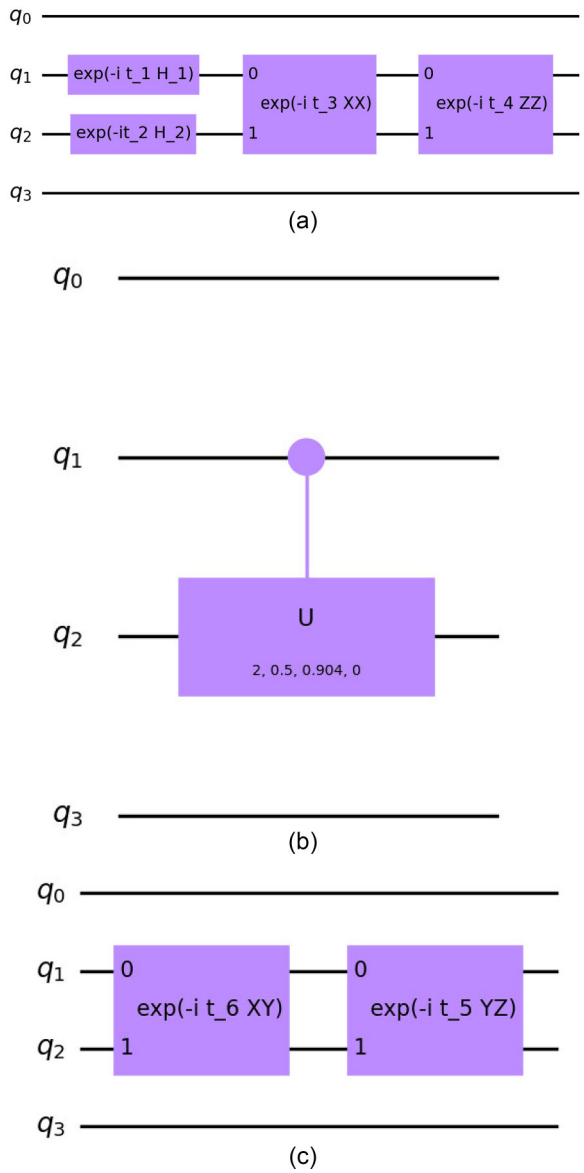

FIG. 9. Circuit diagram of the quantum gates used in the (a) second, (b) third, and (c) fourth rows of Table IV, respectively. (a) $t_1 = \theta^{(2)}_{2,2}/2, t_2 = \theta^{(2)}_{2,3}/2, t_3 = \phi_1, t_4 = \phi_3; H_1 = \vec{\eta}^{(2)}_{2,2} \cdot \vec{\sigma}$ and $H_2 = \vec{\eta}^{(2)}_{2,3} \cdot \vec{\sigma}$. (c) $t_5 = t_6 = \pi/2$. The gates are simulated using the Qiskit software [39].

in literature under the assumption that the parties perform single-qubit unitary operations. In this context, the present findings clearly point out the existence of two-qubit states which failed to generate non-n-locality in the usual linear and nonlinear (star) n-local network but generated the same after being subjected to suitable two-qubit unitary operations (see Table IV). This in turn points out the utility of two-qubit unitary operations in different practical tasks involving quantum network topology.

When the parties perform suitable two-qubit local basis change, the visibility of some classes of bipartite noisy entangled states can increase in the context of generating non-n-locality. Such instances of non-n-locality have been provided for bilocal and star network configuration only. It will be interesting to generalize the study for any n-local quantum network. For that one needs to characterize the correlations lying outside $\mathcal{A}_{\mathcal{I}_\mathcal{T}}$ for any topology $\mathcal{T}$.

It is observed that nontrilocal correlations can be simulated in star-shaped trilocal networks involving a single two-qubit product state. However, even after thorough numerical investigation, no such conclusion can be obtained when more than one pure product state is allowed in such a network. Again, by Theorem 2, it is impossible to get any nontrilocality when each of the sources sends a product state. Regarding $\mathcal{N}_{\text{linear}}$, it is observed that nonbilocality is not detected even if one of the two sources sends a product state. In this context, it will be interesting to analyze the maximum number of two-qubit product states allowed in $\mathcal{N}_{n\text{-star}}$ ($n \geqslant 5$) such that correlations lie outside $\mathcal{A}_{\mathcal{I}_{n\text{-star}}}$.

The present study may be considered as the initial step to exploit the utility of multiqubit unitary operations in $\mathcal{N}_\mathcal{T}$. Here only a few two-qubit unitary operations have been used. These turned out to be sufficient for the purpose of pointing out the effectiveness of suitable local basis change to generate nonbilocal and nontrilocal correlations. However, a detailed analysis of general multiqubit unitary operations in this respect may lead to more interesting findings.

To this end, it may be noted that practical demonstrations of both $\mathcal{N}_{\text{bilocal}}$ and $\mathcal{N}_{3\text{-star}}$ exist in literature [20,44]. In any such network, quantum gates corresponding to the unitary operations may be included. Resulting network architecture may lead to the experimental realization of quantum correlations lying outside $\mathcal{A}_{\mathcal{I}_{\text{bilocal}}}$ and $\mathcal{A}_{\mathcal{I}_{3\text{-star}}}$. However, a detailed discussion of any such experimental setup and practical challenges related to the implementation of the gates in the existing setup lies beyond the scope of the present discussion and can be considered as a direction of future research. Also it will be interesting to establish relations between the entangling capacity of multiqubits gates with that of simulated non-n-local correlations.

APPENDIX A: PROOF OF THEOREM 1

Proof of Theorem 1. For all $i = 1, 2, \ldots, n$, $\mathcal{S}_i$ generates a pure product state:

$$\rho_{i,i+1} = \left[\left(\sum_{j=0}^{1} a_{i,j}|j\rangle\right)\left(\sum_{j=0}^{1} a_{i,j}\langle j|\right)\right] \otimes \left(\sum_{j=0}^{1} b_{i,j}|j\rangle\right)\left(\sum_{j=0}^{1} b_{i,j}\langle j|\right), \quad \text{where } \sum_{j=0}^{1} a^2_{i,j} = \sum_{j=0}^{1} b^2_{i,j} = 1. \tag{A1}$$

The overall state in the network [Eq. (7)] is thus given by

$$\rho_{\text{in}} = \otimes_{i=1}^{n}\left[\left(\sum_{j=0}^{1} a_{i,j}|j\rangle\right)\left(\sum_{j=0}^{1} a_{i,j}\langle j|\right)\right]\otimes_{i=1}^{n}\left[\left(\sum_{j=0}^{1} b_{i,j}|j\rangle\right)\left(\sum_{j=0}^{1} b_{i,j}\langle j|\right)\right]. \tag{A2}$$

Let all the parties perform any possible form of local unitary on their respective share of qubits (see Sec. IV B). The overall state [Eq. (22)] in the network now becomes

$$\rho_f = \otimes_{i=1}^{n+1}\Psi_i, \text{ where} \tag{A3}$$

$$\Psi_1 = \mathcal{U}_1 \cdot \left[\left(\sum_{j=0}^{1} a_{1,j}|j\rangle\right)\left(\sum_{j=0}^{1} a_{1,j}\langle j|\right)\right]\cdot \mathcal{U}_1^{\dagger},$$

$$\Psi_{n+1} = \mathcal{U}_{n+1} \cdot \left[\left(\sum_{j=0}^{1} b_{n,j}|j\rangle\right)\left(\sum_{j=0}^{1} b_{n,j}\langle j|\right)\right]\cdot \mathcal{U}_{n+1}^{\dagger},$$

$$\Psi_k = \mathcal{U}_k \cdot \left[\left(\sum_{j=0}^{1} b_{k-1,j}|j\rangle\right)\left(\sum_{j=0}^{1} b_{k-1,j}\langle j|\right)\right]\otimes\left[\left(\sum_{j=0}^{1} a_{k,j}|j\rangle\right)\left(\sum_{j=0}^{1} a_{k,j}\langle j|\right)\right]\cdot \mathcal{U}_k^{\dagger}\ \forall\, k = 2, 3, \ldots, n. \tag{A4}$$

The parties then perform local measurements on their respective share of qubits, forming ρ_f [Eq. (A3)]. $(n+1)$-partite measurement correlations are used to test the n-local inequality [Eq. (8)]. ρ_f [Eq. (A3)] being the tensor product of single-qubit states Ψ_i, each $(n+1)$-partite correlator term in the n-local inequality [Eq. (8)] can be factorized into the product of single-party correlator terms:

$$\left\langle O_{1,y_1} O_2^i O_3^i \ldots O_{n-1}^i O_{n+1,y_{n+1}}\right\rangle = \langle O_{1,y_1}\rangle \Pi_{j=2}^{n}\left\langle O_j^i\right\rangle\langle O_{n+1,y_{n+1}}\rangle\ \forall\, i = 0, 1. \tag{A5}$$

Observables corresponding to the Bell basis measurement are $\vec{\mathfrak{o}}_j \in \{(1,1),(1,-1),(-1,1),(-1,-1)\}\ \forall\ j = 2, 3, \ldots, n$. So, $|\langle O_j^i\rangle| \leqslant 1\ \forall\ i, j$. Consequently, the L.H.S. of Eq. (8) becomes

$$\begin{aligned}\sqrt{|I_n|} + \sqrt{|J_n|} &\leqslant \frac{1}{2}\sum_{s=0}^{1}\sqrt{|\langle (O_{1,0} + (-1)^s O_{1,1})(O_{n+1,0} + (-1)^s O_{n+1,1})\rangle|}\\ &\leqslant \Pi_{s_1=1,n+1}\sqrt{\frac{\sum_{s_2=0}^{1}|\langle O_{s_1,0} + (-1)^{s_2} O_{s_1,1}\rangle|}{2}}\\ &= \Pi_{s_1=1,n+1}\sqrt{\text{Max}(\langle O_{s_1,0}\rangle, \langle O_{s_1,1}\rangle)} \leqslant 1.\end{aligned} \tag{A6}$$

The inequality in the second line is due to the relation [12]

$$\sum_{j=1}^{n}\left(\Pi_{i=1}^{n} A_{i,j}\right)^{\frac{1}{n}} \leqslant \Pi_{i=1}^{n}\left(\sum_{j=1}^{n} A_{i,j}\right)^{\frac{1}{n}}, \quad A_{i,j} > 0. \tag{A7}$$

Equation (A6) proves the theorem. ■

APPENDIX B: PROOF OF THEOREM 3

Before proving Theorem 3, a lemma is provided.

Lemma 1. Any three-qubit state satisfies the inequality

$$\sum_{s=0}^{1}|\langle O_{1,0}\otimes\sigma_{2+(-1)^s}\otimes\sigma_{2+(-1)^s} + (-1)^s O_{1,1}\otimes\sigma_{2+(-1)^s}\otimes\sigma_{2+(-1)^s}\rangle| \leqslant 2, \tag{B1}$$

where $O_{1,i} = \vec{m}_i\cdot\vec{\sigma}$ $(i = 0, 1)$ with $\vec{m}_i \in \mathfrak{R}_3$.

Proof. Let ϱ be any three-qubit state. Let us first consider the case where ϱ is a pure state. The canonical form of a three-qubit pure state is given by [45]

$$\varrho = |\vartheta\rangle\langle\vartheta|, \text{ where}$$

$$|\vartheta\rangle = \kappa_0|000\rangle + \kappa_1\exp(i\varsigma)|100\rangle + \kappa_2|101\rangle + \kappa_3|110\rangle + \kappa_4|111\rangle, \quad \kappa_i \geqslant 0, 0 \leqslant \varsigma \leqslant \pi, \quad \sum_{i=0}^{4}\kappa_i^2 = 1. \tag{B2}$$

For $i = 0, 1$, let $\vec{m}_i = (\sin\theta_i \cos\beta_i,\ \sin\theta_i \sin\beta_i,\ \cos\theta_i)$. For any three-qubit pure state [Eq. (B2)], the correlator expression in the L.H.S. of Eq. (B1) becomes

$$\begin{aligned}&\left|\left(\kappa_0^2 - \kappa_1^2 + \kappa_2^2 + \kappa_3^2 - \kappa_4^2\right)(\cos\theta_1 + \cos\theta_2) + 2\kappa_0\kappa_1[\cos\varsigma(\cos\beta_1 \sin\theta_1 + \cos\beta_2 \sin\theta_2) + \sin\varsigma(\sin\theta_1 \sin\beta_1 + \sin\theta_2 \sin\beta_2)]\right| \\ &+ |2[-(\kappa_2\kappa_3 + \kappa_1\kappa_4 \cos\varsigma)\cos\theta_1 + (\kappa_2\kappa_3 + \kappa_1\kappa_4 \cos\varsigma)\cos\theta_2 + \kappa_0\kappa_4(\cos\beta_1 \sin\theta_1 - \cos\beta_2 \sin\theta_2)]|. \end{aligned} \tag{B3}$$

Equation (B3) is now maximized over measurement parameters. Applying the inequality $x\cos\theta + y\sin\theta \leqslant (x^2 + y^2)^{1/2}$ for $\theta = \theta_1, \theta_2, \beta_1, \beta_2$, the upper bound of the expression in Eq. (B3) in terms of state parameters is given by

$$\sum_{i=0,1} \sqrt{\left[\kappa_0^2 - \kappa_1^2 + \kappa_2^2 + \kappa_3^2 - \kappa_4^2 + 2(-1)^i(\kappa_2\kappa_3 + \kappa_1\kappa_4 \cos\varsigma)\right]^2 + 4|\kappa_0||\left[\kappa_1 \cos\varsigma + (-1)^{i+1}\kappa_4\right]^2 + \kappa_1^2 \sin^2\varsigma|}. \tag{B4}$$

Maximizing over all the state parameters, maximum value of above expression turns out to be two. Hence, the upper bound of the L.H.S. of Eq. (B1) turns out to be two. This proves the lemma when a three-qubit pure state is considered.

Now any three-qubit mixed state can be written as an ensemble of pure states, $\{\varrho_j, p_j\}_{j=1}^k$. For each ϱ_j, the L.H.S. of Eq. (B1) is $\leqslant 2$. Thus, $2\sum_{j=1}^k p_j \leqslant 2$. This proves the lemma. ■

Proof of Theorem 3. Without loss of generality, let $\mathcal{S}_1$ distribute a two-qubit entangled state ϕ_{ent} and $\mathcal{S}_2$ generate a two-qubit product state [Eq. (A1) for $i = 2$]. After all the parties perform a local basis change, the overall state in the network takes the form

$$\rho_f = \varphi_1 \otimes \varphi_2, \tag{B5}$$

where φ_1 is a three-qubit entangled state shared by parties $\mathcal{P}_1$ and $\mathcal{P}_2$ whereas φ_2 is a single-qubit state of $\mathcal{P}_3$. Owing to this tensor product structure of ρ_f, each tripartite correlator term in the bilocal inequality [Eq. (8) for $n = 2$]

$$\langle O_{1,y_1} O_2^i O_{3,y_3}\rangle = \langle O_{1,y_1} O_2^i\rangle \langle O_{3,y_3}\rangle \ \forall\, i = 0, 1. \tag{B6}$$

Consequently, the L.H.S. of Eq. (8) becomes

$$\begin{aligned}\sqrt{|I_2|} + \sqrt{|J_2|} &= \frac{1}{2}\sum_{s=0}^{1} \sqrt{|\langle\left(O_{1,0}O_2^s + (-1)^s O_{1,1}O_2^s\right)(O_{3,0} + (-1)^s O_{3,1})\rangle|} \\ &\leqslant \sqrt{\frac{\sum_{s=0}^1 |\langle O_{1,0}O_2^s + (-1)^s O_{1,1}O_2^s\rangle|}{2}} \sqrt{\frac{\sum_{s=0}^1 |\langle O_{3,0} + (-1)^s O_{3,1}\rangle|}{2}} \\ &= \sqrt{\frac{\sum_{s=0}^1 |\langle O_{1,0}O_2^s + (-1)^s O_{1,1}O_2^s\rangle|}{2}} \sqrt{\text{Max}(\langle O_{3,0}\rangle, \langle O_{3,1}\rangle)} \\ &\leqslant \sqrt{\frac{\sum_{s=0}^1 |\langle O_{1,0}O_2^s + (-1)^s O_{1,1}O_2^s\rangle|}{2}}\end{aligned} \tag{B7}$$

because observables $O_{3,0}$, $O_{3,1}$ are binary valued. Now, as prescribed in Eq. (8) for $n = 2$, the correlators' expression in the above inequality [Eq. (B7)] is given by

$$\left\langle O_{1,i} O_2^j\right\rangle = \langle \vec{m}_i \cdot \vec{\sigma} \otimes \sigma_{2+(-1)^i} \otimes \sigma_{2+(-1)^j}\rangle \ \forall\, i, j = 0, 1. \tag{B8}$$

Using Eq. (B8) and Lemma 1, in Eq. (B7), the theorem is proved.A. ■

APPENDIX C: PROOF OF THEOREM 4

Proof of Theorem 4. First considering an n-local linear network for proving Eq. (33). As mentioned in the main text, each of the parties is performing imperfect measurements (Table III). Now there exist two correlator terms in the n-local inequality [Eq. (8)]: I_n and J_n. Focusing on the form of expectation terms used in these two correlators gives $\langle O_{1,y_1} O_2^i O_3^i \cdots O_{n-1}^i O_{n+1,y_{n+1}}\rangle$ with $i = 0, 1$ corresponding to I_n and J_n, respectively. The pattern of each of the expectation terms is the same in the sense that each can be interpreted as $W_1 - W_2$ where each of W_1 and W_2 is the linear sum of an equal number of distinct probability terms $p(\mathbf{o}_1, \bar{\mathbf{o}}_2, \ldots, \bar{\mathbf{o}}_{n-1}\mathbf{o}_{n+1}|y_1, y_{n+1}, z_2, \ldots, z_n)$ such that $W_1 + W_2 = 1$. To be more precise, for construction of the expectation terms, the entire set of $(n+1)$-partite probability terms $p(\mathbf{o}_1, \bar{\mathbf{o}}_2, \ldots, \bar{\mathbf{o}}_{n-1}\mathbf{o}_{n+1}|y_1, y_{n+1}, z_2, \ldots, z_n)$ is divided in two groups G_1 and G_2 (say) with $|G_1| = |G_2|$ such that sum of terms from G_i corresponds to $W_i (i = 1, 2)$. Due to such a pattern existing in each of the expectation terms $\langle O_{1,y_1} O_2^i O_3^i \cdots O_{n-1}^i O_{n+1,y_{n+1}}\rangle^{\text{noisy}}$, the contribution of identity operators $(\mathbb{I}_2, \mathbb{I}_2 \otimes \mathbb{I}_2)$ does not appear in the computation of these terms for imperfect measurements [Eq. (21)]. Consequently, the difference between the expectation terms computed in the ideal measurement scenario, in comparison with those in the imperfect scenario lies only in scaling of these terms:

$$\left\langle O_{1,y_1} O_2^i O_3^i \cdots O_{n-1}^i O_{n+1,y_{n+1}}\right\rangle^{\text{noisy}} = \delta_1^{(\text{noise})} \delta_{n+1}^{(\text{noise})} \Pi_{i=2}^n \beta_i^{(\text{noise})} \langle O_{1,y_1} O_2^i O_3^i \cdots O_{n-1}^i O_{n+1,y_{n+1}}\rangle^{\text{ideal}}. \tag{C1}$$

Equation (C1) in turn leads to scaling of the correlator terms I_n and J_n in Eq. (8). This in turn proves the theorem for n-local linear networks.

Consider next $\mathcal{N}_{n\text{-star}}$. For any finite value of n, 2^{n-1} correlator terms appear in the corresponding n-local inequality [Eq. (11)]. The expectation term appearing in each of the correlators depends on $\tilde{\sigma}_1$, which is obtained from classical postprocessing of the raw output string $\overline{\sigma_1}$ of $\mathcal{P}_1$ [12]. As discussed in Ref. [12], each of the expectation terms assumes the same pattern $W_1' - W_2'$ with each of W_1' and W_2' being a linear sum of an equal number of distinct probability terms $p(\tilde{\mathbf{o}}_1\mathbf{o}_2, \ldots, \mathbf{o}_{n+1}|z_1, y_2, \ldots, y_{n+1})$ and $W_1' + W_2' = 1$. So, as discussed for linear networks above, the expectation terms in ideal and imperfect measurement scenarios get related by a scaling factor only:

$$\frac{1}{2^n}\sum_{y_2,\ldots,y_{n+1}}(-1)^{h_i(y_2,\ldots,y_{n+1})}\left\langle A^{(i)}_{(1)}A^{(2)}_{y_2}\cdots A^{(n+1)}_{y_{n+1}}\right\rangle^{\text{noisy}} = \gamma_1^{(\text{noise})}\Pi_{i=2}^{n+1}\delta_i^{(\text{noise})}\frac{1}{2^n}\sum_{y_2,\ldots,y_{n+1}}(-1)^{h_i(y_2,\ldots,y_{n+1})}\left\langle A^{(i)}_{(1)}A^{(2)}_{y_2}\cdots A^{(n+1)}_{y_{n+1}}\right\rangle^{\text{ideal}}. \tag{C2}$$

■

[1] J. S. Bell, Phys. Phys. Fiz. **1**, 195 (1964).
[2] J. S. Bell, *Speakable and Unspeakable in Quantum Mechanics*, 2nd ed. (Cambridge University Press, Cambridge, 2004).
[3] N. Brunner, D. Cavalcanti, S. Pironio, V. Scarani, and S. Wehner, Rev. Mod. Phys. **86**, 419 (2014).
[4] C. M. Lee and M. J. Hoban, Phys. Rev. Lett. **120**, 020504 (2018).
[5] W. Kozlowski and S. Wehner, in *Proceedings of the Sixth Annual ACM International Conference on Nanoscale Computing and Communication, NANOCOM '19* (Association for Computing Machinery, New York, 2019).
[6] W. Dai, T. Peng, and M. Z. Win, IEEE J. Sel. Areas Commun. **38**, C3 (2020).
[7] S. Wehner, D. Elkouss, and R. Hanson, Science **362**, eaam9288 (2018).
[8] C. Branciard, N. Gisin, and S. Pironio, Phys. Rev. Lett. **104**, 170401 (2010).
[9] C. Branciard, D. Rosset, N. Gisin, and S. Pironio, Phys. Rev. A **85**, 032119 (2012).
[10] T. Fritz, New J. Phys. **14**, 103001 (2012).
[11] K. Mukherjee, B. Paul, and D. Sarkar, Quantum Inf. Process. **14**, 2025 (2015).
[12] A. Tavakoli, P. Skrzypczyk, D. Cavalcanti, and A. Acin, Phys. Rev. A **90**, 062109 (2014).
[13] M.-O. Renou, E. Bäumer, S. Boreiri, N. Brunner, N. Gisin, and S. Beigi, Phys. Rev. Lett. **123**, 140401 (2019).
[14] K. Mukherjee, B. Paul, and D. Sarkar, Quantum Inf. Process. **15**, 2895 (2016).
[15] K. Mukherjee, B. Paul, and D. Sarkar, Phys. Rev. A **96**, 022103 (2017).
[16] R. Chaves, Phys. Rev. Lett. **116**, 010402 (2016).
[17] N. Gisin, Q. Mei, A. Tavakoli, M. O. Renou, and N. Brunner, Phys. Rev. A **96**, 020304(R) (2017).
[18] A. Kundu, M. K. Molla, I. Chattopadhyay, and D. Sarkar, Phys. Rev. A **102**, 052222 (2020).
[19] A. Pozas-Kerstjens, N. Gisin, and A. Tavakoli, Phys. Rev. Lett. **128**, 010403 (2022).
[20] F. Andreoli, G. Carvacho, L. Santodonato, M. Bentivegna, R. Chaves, and F. Sciarrino, Phys. Rev. A **95**, 062315 (2017).
[21] F. Andreoli, G. Carvacho, L. Santodonato, R. Chaves, and F. Sciarrino, New J. Phys. **19**, 113020 (2017).
[22] K. Mukherjee, B. Paul, and D. Sarkar, Quantum Inf. Process. **18**, 212 (2019).
[23] K. Mukherjee, B. Paul, and A. Roy, Phys. Rev. A **101**, 032328 (2020).
[24] I. Šupić, J. D. Bancal, and N. Brunner, Phys. Rev. Lett. **125**, 240403 (2020).
[25] A. Tavakoli, N. Gisin, and C. Branciard, Phys. Rev. Lett. **126**, 220401 (2021).
[26] A. Tavakoli, A. Pozas-Kerstjens, M.-X. Luo, and M.-O. Renou, Rep. Prog. Phys. **85**, 056001 (2022).
[27] K. Mukherjee, I. Chakrabarty, and G. Mylavarapu, Phys. Rev. A **107**, 032404 (2023).
[28] K. Mukherjee, S. Mandal, T. Patro, and N. Ganguly, Phys. Rev. A **108**, 032416 (2023).
[29] N. Ganguly, A. Mukherjee, A. Roy, S. S. Bhattacharya, B. Paul, and K. Mukherjee, Int. J. Quantum Inform. **16**, 1850040 (2018).
[30] K. Życzkowski, P. Horodecki, A. Sanpera, and M. Lewenstein, Phys. Rev. A **58**, 883 (1998).
[31] K. Mukherjee, S. Karmakar, B. Paul, and D. Sarkar, Eur. Phys. J. D **73**, 188 (2019).
[32] T. Patro, K. Mukherjee, M. A. Siddiqui, I. Chakrabarty, and N. Ganguly, Eur. Phys. J. D **76**, 127 (2022).
[33] J. F. Clauser, M. A. Horne, A. Shimony, and R. A. Holt, Phys. Rev. Lett. **23**, 880 (1969).
[34] I. Chuang and M. Nielsen, *Quantum Information Science* (Cambridge University Press, Cambridge, England, 2000).
[35] S. Khatri, C. T. Matyas, A. U. Siddiqui, and J. P. Dowling, Phys. Rev. Res. **1**, 023032 (2019).
[36] H. J. Kimble, Nature (London) **453**, 1023 (2008).
[37] S. Luo, Phys. Rev. A **77**, 042303 (2008).
[38] O. Gamel, Phys. Rev. A **93**, 062320 (2016).
[39] Qiskit contributors, Qiskit: An Open-Source Framework for Quantum Computing (2023), 10.5281/zenodo.2573505.
[40] S. Popescu, Phys. Rev. Lett. **74**, 2619 (1995).
[41] A. Wojcik, J. Modlawska, A. Grudka, and M. Czechlewski, Phys. Lett. A **374**, 4831 (2010).
[42] W. Kłobus, W. Laskowski, M. Markiewicz, and A. Grudka, Phys. Rev. A **86**, 020302(R) (2012).
[43] J. P. Ralston, P. Jain, and B. Nodland, Phys. Rev. Lett. **81**, 26 (1998).
[44] D. Poderini, I. Agresti, G. Marchese, E. Polino, T. Giordani, A. Suprano, M. Valeri, G. Milani, N. Spagnolo, G. Carvacho, R. Chaves, and F. Sciarrino, Nat. Commun. **11**, 2467 (2020).
[45] A. Acín, A. Andrianov, L. Costa, E. Jane, J. I. Latorre, and R. Tarrach, Phys. Rev. Lett. **85**, 1560 (2000).